Calculating two-particle correlation functions

R. Lednicky[a,1]

[a] Joint Institute for Nuclear Research, Dubna

The calculation of a two-particle correlation function at small particle momenta in the pair rest frame is described in detail. In particular, the calculation using the exact solutions of the scattering problem at given strong interaction potentials is compared with the approximate one based only on the corresponding scattering amplitudes. The validity of the latter is demonstrated, provided that the characteristic source radius is larger than the range of the two-particle strong interaction.

1. Formalism

It is well known that in a production process of a small enough phase space density (which is usually the case even in heavy-ion collisions) the correlations of two particles emitted with nearly equal four-velocities p_1/M_1 and p_2/M_2 are dominated by their mutual final state interaction (FSI) and, in case of identical particles, also by the symmetrization requirement of quantum statistics (QS).

The FSI and QS effects on two-particle momentum correlations is usually studied with the help of the experimental correlation function $\mathcal{R}^{\rm exp}(p_1,p_2)$, defined as a ratio of the measured momentum distribution of the two particles to the reference one (the latter obtained, e.g., by mixing particles from different events of a given class), normalised to unity at sufficiently large relative momenta [1, 2]:

$$\mathcal{R}^{\rm exp}(p_1,p_2) = N(p_1,p_2)/N^{\rm mix}(p_1,p_2). \tag{1}$$

In fact, the experimental correlation function can be affected by the admixture of misidentified particles or particles from long-lived emitters [3]. Thus, assuming that the true correlation function $\mathcal{R}$ is observed only in a fraction λ of the pairs, while $\mathcal{R} \equiv \widetilde{\mathcal{R}} = 1$ for the remaining fraction $1-\lambda$, one arrives at the experimental correlation function:

$$\mathcal{R}^{\rm exp} = \mathcal{N}[(1-\lambda) + \lambda\mathcal{R}], \tag{2}$$

where $\mathcal{N}$ is a free normalisation parameter.

Often, a possible deviation from unity of the so called residual correlation functions $\widetilde{\mathcal{R}}_i$ [4–6] contributing to the fraction $(1-\lambda) = \sum_i \lambda_i$ of "uncorrelated" pairs is taken into account, modifying Eq. (2) by the substitution

$$(1-\lambda) \to \sum_i \lambda_i \widetilde{\mathcal{R}}_i. \tag{3}$$

[1] E-mail: lednicky@jinr.ru

Also, a momentum dependence is sometimes introduced in the normalisation factor $\mathcal{N}$ to account for possible long-range momentum correlations.

Assuming a smooth behaviour of the single-particle spectra in a narrow region of the correlation effect (smoothness assumption [2]), the theoretical two-particle correlation function can be calculated as [7–9]

$$\mathcal{R}(p_1,p_2) = \tfrac{1}{N(j_1,j_2)} \sum_{m_1 m_2} \sum_{\alpha' m_1' m_2' \ldots} \int d^4x_1' d^4x_2' \ldots$$
$$\cdot G^{\alpha' m_1' m_2' \cdots}(x_1',p_1';x_2',p_2';\ldots) \left| \Psi_{p_1 p_2}^{(-)\alpha m_1 m_2;\alpha' m_1' m_2' \cdots}(x_1',x_2',\ldots) \right|^2 , \tag{4}$$

where $p_i' \doteq PM_i'/(M_1'+M_2'+\ldots)$, j_i' and m_i' are the mean four-momenta, spins and spin projections of the particles in the intermediate channels, $P = p_1+p_2$ is the total four-momentum of the detected particles with the spins j_i and spin projections m_i,

$$N(j_1,j_2) = (2j_1+1)(2j_2+1) \tag{5}$$

is the corresponding number of the spin projections; $\Psi^{(-)\mathcal{J}\mathcal{J}'}$ are the Bethe-Salpeter amplitudes describing transitions from $\mathcal{J}' = \{\alpha' m_1' m_2' \ldots\}$ to $\mathcal{J} = \{\alpha m_1 m_2\}$ channels, properly symmetrized (anti-symmetrized) in case of identical bosons (fermions) with $j_1 = j_2 = j$:

$$\Psi_{p_1 p_2}^{(-)\alpha m_1 m_2;\mathcal{J}'} \to \tfrac{1}{\sqrt{2}} [\Psi_{p_1 p_2}^{(-)\alpha m_1 m_2;\mathcal{J}'} + (-1)^{2j} \Psi_{p_2 p_1}^{(-)\alpha m_2 m_1;\mathcal{J}'}]; \tag{6}$$

$G^{\mathcal{J}'}(x_1',p_1';x_2',p_2';\ldots)$ are the emission functions describing particle emission into the intermediate channels $\mathcal{J}'$ with the mean four-momenta $\{p_1',p_2',\ldots\}$ at the space-time points $\{x_1',x_2',\ldots\}$. The sum is done over the intermediate channel flavours α', the corresponding spin projections $\{m_1' m_2' \ldots\}$ and the spin projections $\{m_1,m_2\}$ of the detected particles with the flavour quantum numbers α. The correlation function (4) is normalised to unity in the absence of FSI and QS, when the Bethe-Salpeter amplitudes of the transitions between different channels vanish and those between the same channels reduce to the product of plane waves: $\Psi^{(-)\mathcal{J}\mathcal{J}'} = \exp(-ip_1x_1' - ip_2x_2')\delta_{\alpha'\alpha}\delta_{m_1' m_1}\delta_{m_2' m_2}$, i.e.

$$\frac{1}{N(j_1,j_2)} \sum_{m_1 m_2} \int d^4x_1' d^4x_2' G^{\alpha m_1 m_2}(x_1',p_1;x_2',p_2) = 1. \tag{7}$$

As for the "smoothness" assumption, it is certainly justified for heavy-ion collisions, being however questionable for electro- or hadro- production processes. In any case, for processes with high numbers of participating particles, the neglect of the space-time coherence in Eq. (4) can be justified based on the statistical concept [10, 11].

Equation (4) assumes that the production time of the particles is much shorter than their interaction time in the final state. For a single-channel FSI, the interaction time is given by the energy derivatives of the phase shifts [12, 13] and becomes very large for s-waves near threshold: $|d\delta_0/dE| = |\mu a_0/k|$, where $\mu = M_1M_2/(M_1+M_2)$ is the reduced mass of the two particles,

k is the particle momentum in the pair rest frame (PRF) and a_0 is the s-wave scattering length. One may thus expect that (4) is valid for k substantially smaller than a typical momentum transfer of a few hundreds MeV/c in the production process, corresponding to the production time of ~ 1 fm/c. If further requiring also the intermediate states not very far from the threshold, i.e. $M_1' + M_2' + \cdots \approx M_1 + M_2$, they practically reduce to the two-particle states with the intermediate particles belonging to the same isospin multiplets as the detected particles. Also, the contribution of multiparticle states with small relative particle velocities is expected to be negligible due to a small or moderate phase-space density of produced particles. Then, $j_i' = j_i$ and the number of the intermediate channels usually reduces to one or two.

In the following, unless it is specified otherwise, we will consider complex multiparticle processes (like those in heavy-ion collisions) implying the equilibration of the spin and isospin projections. The emission function is then independent of these projections. Since particles in the intermediate and final channels are supposed to be the members of the same isospin multiplets, one may substitute the two-particle emission functions $G^{\alpha' m_1' m_2'}(x_1', p_1; x_2', p_2)$ by a universal one [8], $G(x_1', p_1; x_2', p_2)$; here we have omitted its dependence on the channel flavour α. The normalization condition (7) then yields

$$\int d^4x_1 d^4x_2 G(x_1, p_1; x_2, p_2) = 1. \tag{8}$$

Since we consider only processes with a moderate phase space density of produced particles, a free motion of the two-particle c.m. system can be factored out of the Bethe-Salpeter amplitude into the phase factor e^{-iPX}:

$$\Psi^{(-)\mathcal{J}\mathcal{J}'}_{p_1 p_2}(x_1, x_2) = e^{-iPX} \psi^{(-)\mathcal{J}\mathcal{J}'}_{\widetilde{q}}(x), \tag{9}$$

where $X = [(p_1 P)x_1 + (p_2 P)x_2]/P^2$ is the pair c.m. four-coordinate, $x = x_1 - x_2$ is the relative four-coordinate of the emission points, $\widetilde{q} = q - P(qP)/P^2$ is the generalised relative four-momentum of the two detected particles, $q = p_1 - p_2$; in PRF, we have $\mathbf{P} = 0$, $x = \{t, \mathbf{r}\}$, $\widetilde{q} = \{0, 2\mathbf{k}\}$, $\mathbf{k} = \mathbf{p}_1^* = -\mathbf{p}_2^*$. As a result, the correlation function is determined merely by averaging the squares of the reduced Bethe-Salpeter amplitudes $\psi^{(-)\mathcal{J}\mathcal{J}'}_{\widetilde{q}}(x)$ over the distribution $g_P(x, \widetilde{q})$ of the relative four-coordinates of the emission points:

$$\mathcal{R}(p_1, p_2) = \frac{1}{N(j_1, j_2)} \sum_{m_1 m_2} \sum_{\alpha' m_1' m_2'} \int d^4x g_P(x, \widetilde{q}) \cdot \left| \psi^{(-)\alpha m_1 m_2; \alpha' m_1' m_2'}_{\widetilde{q}}(x) \right|^2, \tag{10}$$

$$g_P(x, \widetilde{q}) = \int d^4X G\Big(X + x\frac{(p_2 P)}{P^2}, p_1; X - x\frac{(p_1 P)}{P^2}, p_2\Big), \quad \int d^4x g_P(x, \widetilde{q}) = 1. \tag{11}$$

Note that the reduced equal-time amplitudes in PRF coincide with the complex conjugate of the solutions $\psi^{\mathcal{J}'\mathcal{J}}_{-\mathbf{k}}(\mathbf{r}) \equiv \psi^{(+)\mathcal{J}'\mathcal{J}}_{-\mathbf{k}}(\mathbf{r})$ of the multi-channel scattering problem, having at large $r = |\mathbf{r}|$ the asymptotic form of a superposition of the plane (for $\alpha' = \alpha, m_i' = m_i$) and outgoing spherical waves:

$$\psi^{(-)\mathcal{J}\mathcal{J}'}_{\widetilde{q}}(t = 0, \mathbf{r}) = [\psi^{(+)\mathcal{J}'\mathcal{J}}_{-\widetilde{q}}(t = 0, \mathbf{r})]^* = [\psi^{\mathcal{J}'\mathcal{J}}_{-\mathbf{k}}(\mathbf{r})]^*. \tag{12}$$

Here and below we use the same ψ-notation for the reduced Bethe-Salpeter amplitudes and wave functions with different numbers of the arguments.

Since the scattering process, compared with the production one, corresponds to the opposite time direction, the α-channel three-momentum $\mathbf{k}$ enters in the scattering wave functions $\psi^{(+)}$ with the opposite sign and the detected channel $\alpha = \{1+2\}$ is the entrance scattering channel.

The reduced non-symmetrized Bethe-Salpeter amplitudes $\psi_{\widetilde{q}}^{(-)\mathcal{J}\mathcal{J}'}(x)$ of noninteracting particles are independent of the relative emission time $t = t_1 - t_2$ in PRF: they either coincide with the plane wave $e^{i\mathbf{kr}}$ (for $\mathcal{J}' = \mathcal{J}$) or vanish. On the contrary, the amplitudes of the interacting particles contain an explicit dependence on t which is responsible for vanishing of the FSI at $|t| \to \infty$.

However, it can be shown that the effect of nonequal times on the short-range FSI can be neglected on condition [7, 9]:

$$|t| \ll M(t) r^2, \tag{13}$$

where $M(t > 0) = M_2$ and $M(t < 0) = M_1$. This condition is usually satisfied for heavy particles, like kaons or nucleons. But even for pions, the substitution of the Bethe-Salpeter amplitudes by their values at equal emission times in PRF usually leads to the error in the short-range FSI contribution to the correlation function less than 10% [9].

As for the effect of non-equal times on the Coulomb FSI, it is expected to be rather small as it scales with the two-particle Bohr radius which is usually much larger (some tens or hundreds fm) than a space-time separation of the particle emission points. The effect of the long-range Coulomb FSI is thus practically insensitive to the details of this interaction at small space-time separations. Particularly, for small short-lived systems, the effect of the Coulomb FSI practically factorises in the Coulomb (Gamow) penetration factor - the square of the non-relativistic Coulomb wave function at zero separation (see Section 3):

$$A_{\rm c}(\eta) \equiv |\psi_{-\mathbf{k}}^{\rm Coul}(0)|^2 = 2\pi\eta[\exp(2\pi\eta) - 1]^{-1}, \quad \eta = (ka)^{-1}, \tag{14}$$

where $a = (\mu Z_1 Z_2 e^2)^{-1}$ is the Bohr radius in the channel α consisting of two particles with the reduced mass μ and the electric charges $Z_1 e$ and $Z_2 e$. Note that a is positive (negative) for the repulsive (attractive) Coulomb interaction; e.g., $a = 43.2$ fm for the pd channel.

Adopting the equal-time approximation, Eq. (10) yields

$$\mathcal{R}(p_1, p_2) \doteq \frac{1}{N(j_1, j_2)} \sum_{m_1 m_2} \sum_{\alpha' m_1' m_2'} \int d^3\mathbf{r} W_P(\mathbf{r}, \mathbf{k}) \cdot \left| \psi_{-\mathbf{k}}^{\alpha' m_1' m_2'; \alpha m_1 m_2}(\mathbf{r}) \right|^2, \tag{15}$$

$$W_P(\mathbf{r}, \mathbf{k}) = \int dt g_P(t, \mathbf{r}; 0, 2\mathbf{k}), \quad \int d^3\mathbf{r} W_P(\mathbf{r}, \mathbf{k}) = 1. \tag{16}$$

Passing from the representations $\{m_1 m_2\}$ and $\{m_1' m_2'\}$ of the projections of the particle spins j_1, j_2 and j_1', j_2' to the ones $\{Sm\}$ and $\{S'm'\}$ of the

total channel spins and their projections in the detected and intermediate channels α and α':

$$\psi_{-\mathbf{k}}^{\alpha' m_1' m_2';\alpha m_1 m_2}(\mathbf{r}) = \sum_{Sm} \sum_{S'm'} C_{j_1 m_1; j_2 m_2}^{Sm} C_{j_1 m_1'; j_2 m_2'}^{S'm'} \psi_{-\mathbf{k}}^{\alpha' S' m';\alpha S m}(\mathbf{r}), \qquad (17)$$

one can use the orthonormality of the Clebsch-Gordan coefficients at a fixed projection m of the total spin S,

$$\sum_{m_1 m_2} C_{j_1 m_1; j_2 m_2}^{Sm} C_{j_1 m_1; j_2 m_2}^{\widetilde{S} m} = \delta_{S\widetilde{S}}, \qquad (18)$$

and rewrite (15) as

$$\mathcal{R}(p_1, p_2) = \frac{1}{N(j_1, j_2)} \sum_{Sm} \sum_{\alpha' S' m'} \int d^3\mathbf{r} W_P(\mathbf{r}, \mathbf{k}) \cdot \left| \psi_{-\mathbf{k}}^{\alpha' S' m';\alpha S m}(\mathbf{r}) \right|^2 . \qquad (19)$$

Note that, in the representation of the total spin S, the symmetrization or anti-symmetrization of the scattering wave functions of two identical bosons or fermions in Eq. (6) takes on a common form:

$$\psi_{-\mathbf{k}}^{\alpha' S' m';\alpha S m}(\mathbf{r}) \to \tfrac{1}{\sqrt{2}} \left[\psi_{-\mathbf{k}}^{\alpha' S' m';\alpha S m}(\mathbf{r}) + (-1)^S \psi_{\mathbf{k}}^{\alpha' S' m';\alpha S m}(\mathbf{r}) \right]. \qquad (20)$$

So the wave function of two identical particles with the odd total spin S vanishes at zero relative momentum for both bosons and fermions.

The separation $\mathbf{r}$-distribution can be simulated within various dynamical models or described in terms of simple parameterisations. In a sufficiently narrow interval of the pair three-momenta, it is often characterised by a Gaussian distribution with the radius parameter r_0:

$$W_P(\mathbf{r}, \mathbf{k}) = \frac{1}{(2\sqrt{\pi} r_0)^3} \exp\left(-\frac{r^2}{4 r_0^2} \right), \qquad (21)$$

or - by three Gaussian radii r_{0i}^{LCMS}, $(i = \mathrm{out}, \mathrm{side}, \mathrm{longitudinal})$ in the longitudinally comoving system (LCMS) and a shift $\mathbf{\Delta} = \langle \mathbf{r} \rangle$, which may result from different emission times of nonidentical particles or due to a different collective flow effect on particles with different masses (see [14] and references therein):

$$W_P(\mathbf{r}, \mathbf{k}) = \frac{1}{(2\sqrt{\pi})^3 \prod_i r_{0i}} \exp\left(-\sum_i \frac{(r_i - \Delta_i)^2}{4 r_{0i}^2} \right), \qquad (22)$$

where the PRF radii r_{0i} coincide with the LCMS ones except for the out-radius $r_{0\mathrm{out}} = \gamma_t r_{0\mathrm{out}}^{\mathrm{LCMS}}$; $\gamma_t = (1 - \beta_t^2)^{-1/2}$ is the LCMS Lorentz factor of the pair. At $k \to 0$, the shift vector is practically constant, $\mathbf{\Delta}(\mathbf{k}) \doteq \mathbf{\Delta}_0$, with the vanishing side and longitudinal components provided the analysed sample possesses the azimuthal symmetry and the symmetry with respect to longitudinal reflection, respectively: $\mathbf{\Delta}_0 = \{\Delta_{0\mathrm{out}}, 0, 0\}$, where $\Delta_{0\mathrm{out}} =$

$\langle r_{\rm out}\rangle = \langle \gamma_t (r_{\rm out}^{\rm LCMS} - \beta_t t^{\rm LCMS})\rangle$ is a constant shift in the direction parallel to the pair LCMS three-momentum.

Note that in case of independent particle emission with the same space-time characteristics, the parameter r_0 can be interpreted as a Gaussian radius of the effective particle source, which is nearly at rest in PRF. For different radii r_{01} and r_{02} of the sources of particles 1 and 2, the radius parameter squared is equal to the mean of the radii squared of the two sources:

$$r_0^2 = \left(r_{01}^2 + r_{02}^2\right)/2. \tag{23}$$

2. Momentum correlations of non-interacting identical particles

In the absence of FSI, the symmetrization requirement in Eq. (20) for identical particles takes on the form:

$$\psi_{-\mathbf{k}}^{\alpha' S' m';\alpha S m}(\mathbf{r}) \to \tfrac{1}{\sqrt{2}}\left[e^{-i\mathbf{kr}} + (-1)^S e^{i\mathbf{kr}}\right]\delta_{\alpha'\alpha}\delta_{S'S}\delta_{m'm}. \tag{24}$$

In fact, the symmetrized amplitude form in (24) is valid for any PRF time separation since, for non-interacting particles, the reduced Bethe-Salpeter amplitude $\psi_q^{(-)}(x) = e^{i\mathbf{kr}}$.

Eqs. (10) and (19) then take on the form [2, 7]:

$$\begin{aligned}\mathcal{R}(p_1,p_2) &= \tfrac{1}{N(j_1,j_2)}\textstyle\sum_{Sm}\int d^3\mathbf{r} W_P(\mathbf{r},\mathbf{k})\left[1+(-1)^S\cos(2\mathbf{kr})\right] \\ &= 1 + \textstyle\sum_S \widetilde{\rho}_S (-1)^S \langle\cos(2\mathbf{kr})\rangle,\end{aligned} \tag{25}$$

demonstrating the effect of QS: at small relative momenta $Q = 2k \to 0$, the contribution of the even total spin S in the correlation function is enhanced by a factor of 2, while that of the odd S vanishes.

Here $\widetilde{\rho}_S$ is intrinsic probability of the total spin S in the absence of QS and FSI. In the case of a statistical spin mixture,

$$\widetilde{\rho}_S = \frac{2S+1}{N(j_1,j_2)}, \qquad \sum_S \widetilde{\rho}_S = 1. \tag{26}$$

In case of independent emission of polarised particles, the intrinsic probabilities depend on their polarisation states.

For spin-1/2 fermions, the polarisation state of each fermion is uniquely determined by its intrinsic polarisation vector $\widetilde{\mathbf{P}} = 2\langle\hat{\mathbf{S}}\rangle$, twice the average of the spin operator $\hat{\mathbf{S}}$, and $\widetilde{\rho}_S$ depends on the scalar product of the polarisation vectors of the two fermions [7] :

$$\widetilde{\rho}_0 = \frac{1}{4}\left[1 - \widetilde{\mathbf{P}}(1)\widetilde{\mathbf{P}}(2)\right], \qquad \widetilde{\rho}_1 = \frac{1}{4}\left[3 + \widetilde{\mathbf{P}}(1)\widetilde{\mathbf{P}}(2)\right]. \tag{27}$$

For spin-1 bosons, besides the polarisation vector $\widetilde{\mathbf{P}} = \langle\hat{\mathbf{S}}\rangle$, the polarisation state of each boson is characterised by the symmetric intrinsic polarisation tensor $\widetilde{T}_{ij} = \langle 3\hat{S}_i\hat{S}_j - 2\delta_{ij}\rangle$, $i,j = x,y,z$, entering in $\widetilde{\rho}_S$ through their

Frobenius inner (scalar) product:

$$\left(\widetilde{T}(1),\widetilde{T}(2)\right)_F=\sum_i\widetilde{T}_i(1)\widetilde{T}_i(2)+2\sum_{i\neq j}\widetilde{T}_i(1)\widetilde{T}_j(2), \tag{28}$$

$$\widetilde{\rho}_0=\tfrac{1}{9}\left[1-\tfrac{3}{2}\widetilde{\mathbf{P}}(1)\widetilde{\mathbf{P}}(2)+\tfrac{1}{3}\left(\widetilde{T}(1),\widetilde{T}(2)\right)_F\right],$$

$$\widetilde{\rho}_1=\tfrac{1}{9}\left[3-\tfrac{9}{4}\widetilde{\mathbf{P}}(1)\widetilde{\mathbf{P}}(2)-\tfrac{1}{2}\left(\widetilde{T}(1),\widetilde{T}(2)\right)_F\right], \tag{29}$$

$$\widetilde{\rho}_2=\tfrac{1}{9}\left[5+\tfrac{15}{4}\widetilde{\mathbf{P}}(1)\widetilde{\mathbf{P}}(2)+\tfrac{1}{6}\left(\widetilde{T}(1),\widetilde{T}(2)\right)_F\right].$$

As for the correlation term $\langle\cos(2\mathbf{kr})\rangle$, for the product of the Gaussians in Eq. (22) with $\Delta_i=0$ and dispersions $\langle r_i^2\rangle=2r_{0i}^2$, one has

$$\langle\cos(2\mathbf{kr})\rangle=\exp\left(-\sum_i r_{0i}^2Q_i^2\right)\ \ \rightarrow\ \ \exp(-r_0^2Q^2), \tag{30}$$

where the arrow indicates the result corresponding to a spherically symmetrical Gaussian in Eq. (21) with the dispersions $\langle {r_i}^2\rangle=2r_0^2$.

For a spherically symmetrical Gaussian $\mathbf{r}$-distribution (21), Eqs. (25), (27)-(30) yield for the experimental correlation function in Eq. (2):

$$\mathcal{R}^{\rm exp}=\mathcal{N}\left[1+\lambda c_j\exp(-r_0^2Q^2)\right], \tag{31}$$

where c_j is a positive (negative) number for spin-j bosons (fermions). E.g., $c_0=1$, $c_{1/2}=-\frac{1}{2}(1+\widetilde{\mathbf{P}}^2)$ and $c_2=\frac{1}{3}[1+\frac{3}{2}\widetilde{\mathbf{P}}^2+\frac{1}{3}(\widetilde{T},\widetilde{T})_F]$, assuming $\widetilde{\mathbf{P}}(i)=\widetilde{\mathbf{P}}$ and $\widetilde{T}(i)=\widetilde{T}$ at small Q. The QS correlation at small Q thus leads to a spike (dip) of a width $1/r_0$ in the correlation function of two bosons (fermions).

3. Coulomb FSI effect on two-particle momentum correlations

In the absence of short-range FSI, the scattering wave function matrix $\widehat{\psi}_{-\mathbf{k}}$ is practically diagonal in spin projections and channel flavours. Thus, for two charged particles, neglecting a weak spin dependence of the Coulomb interaction, one has:

$$\psi_{-\mathbf{k}}^{\alpha' S' m';\alpha S m}(\mathbf{r})=\psi_{-\mathbf{k}}^{\alpha;\rm Coul}(\mathbf{r})\delta_{\alpha'\alpha}\delta_{S'S}\delta_{m'm}, \tag{32}$$

$$\psi_{-\mathbf{k}}^{\alpha;\rm Coul}(\mathbf{r})=e^{i\sigma_0(\eta)}(A_{\rm c}(\eta))^{1/2}e^{-i\mathbf{kr}}F(-i\eta,1,i\zeta), \tag{33}$$

where $\sigma_0(\eta)=\arg\Gamma(1+i\eta)$ is the Coulomb s-wave phase shift,

$$F(x,1,z)=1+xz/1!^2+x(x+1)z^2/2!^2+\ldots \tag{34}$$

is the confluent hypergeometric function, $\zeta=kr+\mathbf{kr}=kr(1+\cos\theta)$ and the Coulomb (Gamow) penetration factor $A_{\rm c}(\eta)$ is defined in (14). Here

and below the quantities with the omitted channel indices correspond to the channel flavour α.

In the absence of the Coulomb interaction, we have $|a| = \infty$, $\eta = 0$, $A_c(0) = 1$, $\sigma_0(0) = 0$, $F(0, 1, i\zeta) = 1$ and the pure Coulomb wave function $\psi^{\alpha;\mathrm{Coul}}_{-\mathbf{k}}(\mathbf{r})$ coincides with the plane wave $e^{-i\mathbf{kr}}$.

Inserting the Coulomb wave function (33) into Eqs. (19) and (20), one gets the correlation function due to a pure Coulomb FSI:

$$\mathcal{R}^{\mathrm{Coul}}(k) = A_c(\eta) \left\langle |F(-i\eta, 1, i\zeta)|^2 \right\rangle \tag{35}$$

for non-identical particles and

$$\mathcal{R}^{\mathrm{Coul}}(k) = \frac{1}{2} A_c(\eta) \left\langle |F_+|^2 + F_-|^2 + 2 \sum_S \widetilde{\rho}_S (-1)^S \Re \left(e^{-2i\mathbf{kr}} F_+ F_-^* \right) \right\rangle \tag{36}$$

for identical particles, where $F_\pm = F(-i\eta, 1, i\zeta_\pm)$, $\zeta_\pm = kr(1 \pm \cos\theta)$.

One may see from Eqs. (33)-(36) that, at a mean r-separation much smaller than the Bohr radius $|a|$, the pure Coulomb correlation function of two non-identical charged particles coincides with the Coulomb (Gamow) factor $A_c(\eta)$ and that, for two identical charged particles, the Coulomb FSI effect reduces to multiplication of the pure QS correlation function in Eq. (25) by $A_c(\eta)$.

It has been shown [15] that the Coulomb effect on the correlation function of identical charged pions can be, with a reasonable accuracy, factored out in a generalised Coulomb factor $\tilde{A}_c(\eta, \langle r \rangle)$, depending on the mean r-separation. This factor can be identified with a pure Coulomb correlation function in Eq. (35) for the particles considered as non-identical. Such an approximate factorisation of the Coulomb effect, valid up to $O(\langle r \rangle^2 / a^2)$, is widely used to extract the pion femtoscopic radii from correlation functions of two identical charged pions, characterised by a large Bohr radius of 387.5 fm.

Fig. 1 demonstrates the k-dependence of the pure Coulomb proton-deuteron correlation function, changing from 1 to $A_c(\eta)$ for the Gaussian source radii r_0 ranging from ∞ to 0. One may see that in the classical region $k\langle r \rangle \gg 1$, the pure Coulomb correlation function approaches unity with increasing k as [9] $1 - \langle r^{-1} \rangle / (ak^2)$, i.e. much faster than the quantum factor $A_c(\eta) \to 1 - \pi/(ak)$); note that $\langle r^{-1} \rangle = (\sqrt{\pi} r_0)^{-1}$ for the Gaussian $\mathbf{r}$-distribution in Eq. (21).

4. Treating the angular dependence

Near threshold, only the lowest values of the orbital angular momenta contribute. It is thus convenient to introduce the complete sets $\{L, L_z\}$ and $\{L', L'_z\}$ in the entrance and exit channels. Directing the quantization axis $\hat{\mathbf{z}}$ parallel to $\mathbf{k} = k(0, 0, 1) = k\hat{\mathbf{z}}$ and introducing the polar (θ) and azimuthal (ϕ) angles of the vector $\mathbf{r} = r(\sin\theta\cos\phi, \sin\theta\sin\phi, \cos\theta) = r\hat{\mathbf{r}}$, one can express the angular dependence of the wave functions at given $\{L, L_z\}$

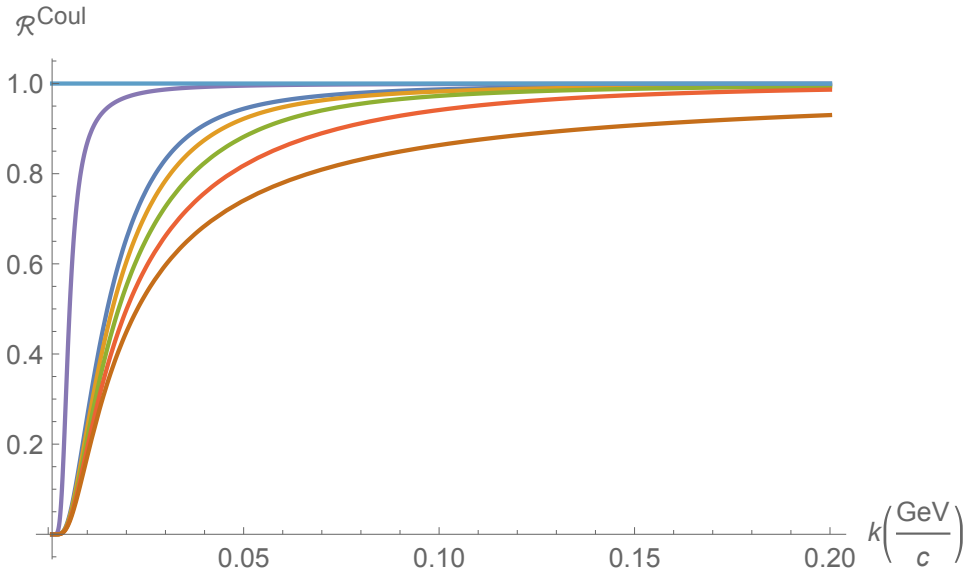

Fig. 1. The pure Coulomb proton-deuteron correlation functions $\mathcal{R}^{\mathrm{Coul}}(k)$ calculated according to Eq. (35). In decreasing order, they correspond to the Gaussian source radii $r_0 = \infty$, 43.2, 4, 3, 2, 1.5 and 0 fm; note that the proton-deuteron Bohr radius $a = 43.2$ fm.

and $\{L', L'_z\}$ through the Wigner D-functions - the matrix elements of the rotations from the direction of a quantization axis $\hat{\mathbf{z}} = \hat{\mathbf{k}}$ to the directions of vectors $\mathbf{r}$ and $-\mathbf{k}$:

$$\begin{aligned}\psi^{\alpha' S' m';\alpha S m}_{-\mathbf{k}}(\mathbf{r}) &= \textstyle\sum_{LL_zL'L'_z}[(2L'+1)(2L+1)]^{1/2}\psi^{\alpha' S' m';\alpha S m}_{k;L'L'_zLL_z}(r) \\ &\qquad \cdot D^{L'*}_{L'_z,0}(\phi,\theta,0)D^{L}_{L_z,0}(\pi,\pi,0) \\ &= \textstyle\sum_{LL'}[(2L'+1)(2L+1)]^{1/2}\psi^{\alpha' S' m';\alpha S m}_{k;L'L}(r) \\ &\qquad \cdot (-1)^L D^{L'*}_{m-m',0}(\phi,\theta,0).\end{aligned} \tag{37}$$

The second equality follows from vanishing of the $\mathbf{L}$ projection on the direction $-\hat{\mathbf{k}}$: $D^{L}_{L_z,0}(\pi,\pi,0) = (-1)^L\delta_{L_z0}$, and - conservation of the projection of the total angular momentum $\mathbf{J} = \mathbf{L} + \mathbf{S}$: $L'_z + m' = L_z + m = m$.

As for the scattering wave function $\psi^{\alpha' S' m';\alpha S m}_{\mathbf{k}}$, entering in symmetrized wave function (20) for identical particles, it is given by Eq. (37) with the substitutions $D^{L}_{L_z,0}(\pi,\pi,0) \to D^{L}_{L_z,0}(0,0,0) = \delta_{L_z0}$ and $(-1)^L \to 1$ in the first and second equalities, respectively. The symmetrized wave function then becomes

$$\begin{aligned}\psi^{\alpha' S' m';\alpha S m}_{-\mathbf{k}}(\mathbf{r}) &\to \textstyle\sum_{LL'}[(2L'+1)(2L+1)]^{1/2}\psi^{\alpha' S' m';\alpha S m}_{k;L'L}(r) \\ &\qquad \cdot (-1)^L \tfrac{1}{\sqrt{2}}\left[1+(-1)^{L+S}\right] D^{L'*}_{m-m',0}(\phi,\theta,0),\end{aligned} \tag{38}$$

with non-vanishing contributions for even $(L+S)$ only.

Here we use the PDG convention for the D-matrix so that it coincides with the Hermitian conjugate Wigner D-matrix. The D-matrix elements are related to the spherical harmonics $Y_{L'}^{L'_z}$ as:

$$D^{L'*}_{L'_z,0}(\phi,\theta,0) = e^{iL'_z\phi} d^{L'}_{L'_z,0}(\theta) = \left(\tfrac{4\pi}{2L'+1}\right)^{1/2} Y^{L'_z}_{L'}(\theta,\phi); \tag{39}$$

particularly, $d^{L'}_{00}(\theta)$ coincides with the Legendre polynomial $P_{L'}(\cos\theta)$.

Note that the correlation function (19) is independent of the azimuthal angle, which enters through the phase factors $e^{i(m-m')\phi}$ only and vanishes in the wave functions squared.

Finally, using the independence of the wave functions on the projections of the conserved total angular momentum $\mathbf{J} = \mathbf{L} + \mathbf{S}$ (following from the rotation invariance), the dependence on the projections m, m' of the total spins S, S' can be separated in the Clebsch-Gordan coefficients of the L-S addition:

$$\psi^{\alpha' S' m';\alpha S m}_{k;L'L}(r) = \sum_J C^{Jm}_{L0;Sm} C^{Jm}_{L'm-m';S'm'} \psi^{\alpha'\alpha;J}_{k;L'S'LS}(r). \tag{40}$$

The situation is greatly simplified near scattering threshold, when central forces usually dominate and both the orbital angular momentum L and the total spin S are practically conserved:

$$\psi^{\alpha'\alpha;J}_{k;L'S'LS}(r) \doteq \psi^{\alpha'\alpha;J}_{k;LS}(r)\delta_{L'L}\delta_{S'S}. \tag{41}$$

Eq. (40) then reduces to

$$\begin{aligned} \psi^{\alpha' S' m';\alpha S m}_{k;L'L}(r) &\doteq \psi^{\alpha'\alpha;m'm}_{k;LS}(r)\delta_{L'L}\delta_{S'S} \\ \psi^{\alpha'\alpha;m'm}_{k;LS}(r) &= \textstyle\sum_J \psi^{\alpha'\alpha;J}_{k;LS}(r) C^{Jm}_{L0;Sm} C^{Jm}_{Lm-m';Sm'} \end{aligned} \tag{42}$$

and Eq, (37) - to

$$\begin{aligned} \psi^{\alpha' S' m';\alpha S m}_{-\mathbf{k}}(\mathbf{r}) &\doteq \psi^{\alpha'\alpha;m'm}_{-\mathbf{k};S}(\mathbf{r})\delta_{S'S} \\ \psi^{\alpha'\alpha;m'm}_{-\mathbf{k};S}(\mathbf{r}) &= \textstyle\sum_L (2L+1)\psi^{\alpha'\alpha;m'm}_{k;LS}(r)(-1)^L D^{L*}_{m-m',0}(\phi,\theta,0) \\ &= \textstyle\sum_{LJ}(2L+1) C^{Jm}_{L0;Sm} C^{Jm}_{Lm-m';S'm'} \psi^{\alpha'\alpha;J}_{k;LS}(r) \\ &\quad \cdot (-1)^L D^{L*}_{m-m',0}(\phi,\theta,0), \end{aligned} \tag{43}$$

Note that the total spin S is conserved in nucleon-nucleon (nucleon-antinucleon) elastic scattering as a consequence of quantum statistics (charge conjugation symmetry) and time-reversal symmetry, in addition to parity conservation and isospin invariance.

If further neglecting the total angular momentum (J) splitting of the scattering wave functions and using

$$\sum_J C^{Jm}_{L0;Sm} C^{Jm}_{Lm-m';Sm'} = \delta_{mm'}, \tag{44}$$

Eq. (43) reduces to

$$\begin{aligned}\psi^{\alpha'\alpha;m'm}_{-\mathbf{k};;S}(\mathbf{r}) &\approx \psi^{\alpha'\alpha}_{-\mathbf{k};S}(\mathbf{r})\delta_{m'm} \\ &= \textstyle\sum_L (2L+1)\psi^{\alpha'\alpha}_{k;LS}(r)(-1)^L P_L(\cos\theta)\delta_{m'm},\end{aligned} \tag{45}$$

guaranteeing, besides the LS-conservation, also independence of the scattering wave functions on the total spin S projections.

Note that Eq. (45) was assumed in proton-deuteron phase shift analysis in [16] and a weak J-splitting near pd threshold was confirmed in [17], contrary to a significant J-splitting in nucleon-nucleon scattering [18].

In case of the scattering wave functions independent of the total spin S projections (e.g., due to a weak J-splitting or due to a dominant s-wave short-range interaction), the correlation function (19) takes on simple forms:

$$\begin{aligned}\mathcal{R}(p_1,p_2) &\approx \textstyle\sum_{\alpha' S} \widetilde{\rho}_S \int d^3\mathbf{r} W_P(\mathbf{r},\mathbf{k}) \left|\psi^{\alpha'\alpha}_{-\mathbf{k};S}(\mathbf{r})\right|^2 \\ &\to \textstyle\sum_{\alpha' SL} \widetilde{\rho}_S (2L+1) \left\langle \left|\psi^{\alpha'\alpha}_{k;LS}(r)\right|^2 \right\rangle\end{aligned} \tag{46}$$

for non-identical particles and

$$\begin{aligned}\mathcal{R}(p_1,p_2) &\approx \tfrac{1}{2}\textstyle\sum_{\alpha' S} \widetilde{\rho}_S \int d^3\mathbf{r} W_P(\mathbf{r},\mathbf{k}) \left|\psi^{\alpha'\alpha}_{-\mathbf{k};S}(\mathbf{r}) + (-1)^S \psi^{\alpha'\alpha}_{\mathbf{k};S}(\mathbf{r})\right|^2 \\ &\to 2\textstyle\sum_{\alpha'} \sum_{(S+L)-\text{even}} \widetilde{\rho}_S (2L+1) \left\langle \left|\psi^{\alpha'\alpha}_{k;LS}(r)\right|^2 \right\rangle\end{aligned} \tag{47}$$

for identical particles. The arrows indicate results of the angular averaging in case of a spherically symmetric $\mathbf{r}$-distribution $W_P(\mathbf{r},\mathbf{k})$ (like in Eq. (21)); these results follow from Eq. (45), the orthogonality of the d-functions:

$$\int_{-1}^{1} d\cos\theta d^L_{\mu\nu}(\theta) d^{\widetilde{L}}_{\mu\nu}(\theta) = \frac{2}{2L+1}\delta_{L\widetilde{L}} \tag{48}$$

and the relation $d^L_{00}(\theta) = P_L(\cos\theta)$.

The intrinsic probabilities $\widetilde{\rho}_S$ of the total spin S are given in Eq. (26) in case of a statistical spin mixture, or in Eqs. (27), (29) with $\widetilde{\mathbf{P}}(i) \to \widetilde{\mathbf{P}}_i, \widetilde{T}(i) \to \widetilde{T}_i$ in case of independent production of polarised particles for $j_1 = j_2 = 1/2$, $j_1 = j_2 = 1$ and

$$\widetilde{\rho}_{1/2} = \frac{1}{3}\left[1 - \widetilde{\mathbf{P}}_1\widetilde{\mathbf{P}}_2\right], \quad \widetilde{\rho}_{3/2} = \frac{1}{3}\left[2 + \widetilde{\mathbf{P}}_1\widetilde{\mathbf{P}}_2\right] \tag{49}$$

for $j_1 = 1/2, j_2 = 1$ (e.g., for pd pair).

A similar single-channel form of Eq. (46) was used in [19] to calculate the two-proton correlation function of the protons emitted with non-relativistic momenta in the source rest frame, taking into account the short-range interaction up to d-waves. To account for the J-splitting of the triplet waves, the

appropriate incoherent average over initial and final spin projections m and m' was done like in Eq. (19). In fact, at $k < 50 - 100$ MeV/c, it is often sufficient to account for the short-range nucleon-nucleon interaction in the s-waves only [7, 19], which are independent of the total spin S projections since then they coincide with those of the total angular momentum $J = S$.

Using Eq. (48), the angular averaging of the general form (19) of the correlation function for a spherically symmetric $\mathbf{r}$-distribution yields for non-identical particles:

$$\mathcal{R}(p_1,p_2) \to \sum_{Sm}\sum_{\alpha' S' m'}\sum_{L\widetilde{L}L'} \tfrac{[(2L+1)(2\widetilde{L}+1)]^{1/2}}{N(j_1,j_2)}(-1)^{L+\widetilde{L}} \cdot \left\langle \psi^{\alpha' S' m';\alpha S m}_{k;L'L}(r)\psi^{\alpha' S' m';\alpha S m*}_{k;L'\widetilde{L}}(r)\right\rangle \quad (50)$$

$$= \sum_{SL}\sum_{\alpha' S' L'}\sum_{J=\max(|L'-S'|,|L-S|)}^{\min(L'+S',L+S)} \tfrac{2J+1}{N(j_1,j_2)}\left\langle \left|\psi^{\alpha'\alpha;J}_{k;L'S'LS}(r)\right|^2\right\rangle;$$

the second expression follows from the relations

$$\sum_{m'} C^{Jm}_{L'm-m'S'm'}C^{\widetilde{J}m}_{L'm-m'S'm'} = \delta_{\widetilde{J}J}, \quad \sum_{m} C^{Jm}_{L0Sm}C^{Jm}_{\widetilde{L}0Sm} = \frac{2J+1}{2L+1}\delta_{\widetilde{L}L}. \quad (51)$$

In case of the LS-conservation, Eqs. (19) and (50) are simplified to:

$$\mathcal{R}(p_1,p_2) \doteq \tfrac{1}{N(j_1,j_2)}\sum_{\alpha' S}\sum_{m'm}\int d^3\mathbf{r} W_P(\mathbf{r},\mathbf{k})\left|\psi^{\alpha'\alpha;m'm}_{-\mathbf{k};S}(\mathbf{r})\right|^2$$

$$\to \sum_{\alpha' SL}\sum_{m'm}\tfrac{2L+1}{N(j_1,j_2)}\left\langle\left|\psi^{\alpha'\alpha;m'm}_{k;LS}(r)\right|^2\right\rangle \quad (52)$$

$$= \sum_{\alpha' SL}\sum_{J=|L-S|}^{L+S}\tfrac{2J+1}{N(j_1,j_2)}\left\langle\left|\psi^{\alpha'\alpha;J}_{k;LS}(r)\right|^2\right\rangle.$$

Eq. (52) reduces to (46) on the absence of the J-splitting, since

$$\sum_{J=|L-S|}^{L+S}\frac{2J+1}{N(j_1,j_2)} = \frac{(2L+1)(2S+1)}{N(j_1,j_2)} = (2L+1)\widetilde{\rho}_S, \quad (53)$$

where the last equality follows from Eq. (26) for ρ_S in case of the statistical spin mixture.

For identical particles, the correlation functions in Eqs. (50) and (52) for a spherically symmetric $\mathbf{r}$-distribution should be multiplied by 2 and summing done for even $(\tilde{L}+S)$ and $(L+S)$ only.

5. Calculation details

5.1. Contribution of the outer region

5.1.1. Treating the Coulomb and strong interaction One may introduce separation parameter $\epsilon > d$ to split the correlation function in the outer ($r > \epsilon$) and inner ($r \leq \epsilon$) contributions: $\mathcal{R} = \mathcal{R}_{>\epsilon} + \mathcal{R}_{<\epsilon}$. Outside the range of the strong interaction potential, $r > \epsilon > d$, the scattering wave functions are independent of the actual potential form and can be analytically expressed through the corresponding scattering amplitudes [7, 20]. In the considered case of the LS-conservation, one then has for $r > d$:

$$\begin{aligned} \psi^{\alpha'\alpha;m'm}_{k;LS}(r) &= \widetilde{\psi}^{\alpha'\alpha;m'm}_{k;LS}(r) \\ &= e^{i\sigma_L(\eta_\alpha)} i^L \left[\frac{F_L(\eta_\alpha,\rho_\alpha)}{\rho_\alpha} \delta_{\alpha'\alpha}\delta_{m'm} + \left(\frac{\mu_{\alpha'}}{\mu_\alpha}\right)^{1/2} k_{\alpha'} f^{\alpha'\alpha;m'm}_{k;LS} \frac{H_L(\eta_{\alpha'},\rho_{\alpha'})}{\rho_{\alpha'}} \right], \end{aligned} \tag{54}$$

where $\rho_{\alpha'} = k_{\alpha'} r$ and $\eta_{\alpha'} = (k_{\alpha'} a_{\alpha'})^{-1}$ is defined as in (14) with the two-particle Bohr radius $a_{\alpha'}$ in the channel α' and channel momentum $k_{\alpha'} = k_{\alpha'}(k)$; the function $H_L(\eta,\rho) = G_L(\eta,\rho) + iF_L(\eta,\rho)$ is a Hankel type combination of the regular (F_L) and singular (G_L) Coulomb functions at a given orbital angular momentum L, σ_L is the Coulomb L-wave phase shift:

$$\sigma_L(\eta) = \arg\Gamma(L+1+i\eta) = \sigma_0(\eta) + \sum_{l=1}^{L} \arctan\frac{\eta}{l}; \tag{55}$$

$\mu_{\alpha'}$ is the relativistic generalisation of the reduced mass: $\mu_{\alpha'} = E'_1 E'_2/(E'_1 + E'_2)$, where $E'_i = (M'^2_i + k^2_{\alpha'})^{1/2}$, $E'_1 + E'_2 = E_1 + E_2 \equiv E$; $\mu_{\alpha'} = E/2$ for particles with equal masses.

The dependance of the scattering amplitudes on the total spin S projections can be factored out in the Clebsch-Gordan coefficients of the L-S addition as in Eq. (42):

$$f^{\alpha'\alpha;m'm}_{k;LS}(r) = \sum_J C^{Jm}_{L0;Sm} C^{Jm}_{Lm-m';Sm'} f^{\alpha'\alpha;J}_{k;LS}(r), \tag{56}$$

For practical calculations, it is convenient to perform the summation over L in the pure Coulomb part of the wave function (43) analytically:

$$\psi^{\alpha;\mathrm{Coul}}_{-\mathbf{k}}(\mathbf{r}) = \sum_{L=0}^{\infty} (2L+1) i^L e^{i\sigma_L(\eta)} \frac{F_L(\eta,\rho)}{\rho} (-1)^L P_L(\cos\theta), \tag{57}$$

where the pure Coulomb wave function $\psi^{\alpha;\mathrm{Coul}}_{-\mathbf{k}}(\mathbf{r})$ is expressed through the confluent hypergeometric function $F[-i\eta, 1, \rho(1+\cos\theta)]$ in Eq. (33). Then, one can rewrite the wave function in the outer region as

$$\begin{aligned} \widetilde{\psi}^{\alpha'\alpha;m'm}_{-\mathbf{k};S}(\mathbf{r}) = \psi^{\alpha;\mathrm{Coul}}_{-\mathbf{k}}(\mathbf{r}) \delta_{\alpha'\alpha}\delta_{m'm} + \textstyle\sum_L (2L+1) i^L e^{i\sigma_L(\eta_\alpha)} \left(\frac{\mu_{\alpha'}}{\mu_\alpha}\right)^{1/2} \\ \cdot k_{\alpha'} f^{\alpha'\alpha;m'm}_{k;LS} \frac{H_L(\eta_{\alpha'},\rho_{\alpha'})}{\rho_{\alpha'}} (-1)^L D^{L*}_{m-m',0}(\phi,\theta,0). \end{aligned} \tag{58}$$

Note that the wave function representation (58) was first used in [7] to account for the effect of the single-channel short-range FSI on correlation functions near threshold in the s-wave approximation and generalised to the multi-channel case in [8].

In the absence of the Coulomb interaction, we have $\eta = 0$, $\sigma_L(0) = 0$, $F_L(0,\rho) = S_L(\rho)$, $G_L(0,\rho) = C_L(\rho)$, $H_L(0,\rho) = h_L(\rho) \equiv C_L(\rho) + iS_L(\rho)$ and

$$\psi^{\alpha;\mathrm{Coul}}_{-\mathbf{k}}(\mathbf{r}) = e^{-i\mathbf{kr}} = \sum_{L=0}^{\infty}(2L+1)i^L j_L(\rho)(-1)^L P_L(\cos\theta). \tag{59}$$

The Riccati-Bessel functions S_L and C_L are simply related to the spherical Bessel functions j_L and y_L of the first and second kind, respectively: $S_L(\rho) = \rho j_L(\rho)$ and $C_L(\rho) = -\rho y_L(\rho)$. Their combination $h_L(\rho) = i\rho h^{(1)}_L(\rho)$, where $h^{(1)}_L(\rho)$ is the spherical Hankel function of the first kind; $h_L(\rho) \to e^{i(\rho - L\pi/2)}$ at $\rho \to \infty$ and, particularly, for $L = 0, 1, 2$:

$$h_0(\rho) = e^{i\rho}, \quad h_1(\rho) = e^{i\rho}\left(\frac{1}{\rho} - i\right), \quad h_2(\rho) = e^{i\rho}\left(\frac{3}{\rho^2} - \frac{3i}{\rho} - 1\right). \tag{60}$$

In single-channel case, absent J-splitting and absent Coulomb interaction, Eqs. (45) and (58) yield in the outer region:

$$\begin{aligned}\widetilde{\psi}^{m'm}_{k;LS}(\mathbf{r}) &= e^{i\delta_{LS}}\left[j_L(\rho)\cos\delta_{LS} - y_{LS}\sin\delta_{LS}\right]\delta_{m'm} \\ &\to e^{i\delta_{LS}}\sin\left(\rho + \delta_{LS} - L\pi/2\right)\delta_{m'm}/\rho,\end{aligned} \tag{61}$$

where the arrow indicates the limit $\rho \to \infty$.

5.1.2. Treating the isospin and multi-channel unitarity One can consider the scattering amplitudes $f^{\alpha'\alpha;J}_{k;LS}$ as the elements of the scattering amplitude matrix in the channel flavour representation, satisfying the matrix unitarity condition:

$$\Im\hat{f}^J_{LS} = \hat{f}^{J+}_{LS}\Re\hat{k}\hat{f}^J_{LS}, \tag{62}$$

where $\hat{k}$ is the diagonal matrix formed by the channel momenta $k_{\alpha'}$: $k_{\alpha'\alpha''} = k_{\alpha'}\delta_{\alpha'\alpha''}$; here and below, the amplitude dependence on the α-channel momentum k is omitted: $f^{\alpha'\alpha;J}_{k;LS} \equiv f^{\alpha'\alpha;J}_{LS}$.

The invariance with respect to the time reflection requires the symmetry of the amplitude matrix: $f^{\alpha'\alpha'';J}_{LS} = f^{\alpha''\alpha';J}_{LS}$.

In the case of a single channel α near threshold (e.g., $\alpha = \pi^+K^+$, π^+p or pd), the unitarity condition (62) allows one to express the amplitudes $f^J_{LS} \equiv f^{\alpha\alpha;J}_{LS}$ through the phase shifts $\delta^J_{LS} \equiv \delta^{\alpha\alpha;J}_{LS}$:

$$f^J_{LS} = \frac{e^{2i\delta^J_{LS}} - 1}{2ik} = \left(k\cot\delta^J_{LS} - ik\right)^{-1} = \frac{1}{k}e^{i\delta^J_{LS}}\sin\delta^J_{LS}. \tag{63}$$

Sufficiently far above the threshold, when the isospin violation induced by Coulomb interaction can be neglected, one can express the elements of

the amplitude matrix in the channel flavour representation through the elements of the diagonal amplitude matrix in the representation of the conserved channel isospin T:

$$f_{LS}^{\alpha'\alpha;J} = \sum_T C^{Tt}_{T_1t_1;T_2t_2} C^{Tt}_{T_1t'_1;T_2t'_2} f_{LS}^{T;J}, \tag{64}$$

where T_i and t'_i are the i-th particle isospin and its projection in the channel with flavour α'.

Thus, for the channels $\alpha = \{\pi^-K^+, \pi^+K^-, \pi^-p, \pi^+\Xi^-\}$ and the corresponding ones $\beta = \{\pi^0K^0, \pi^0\bar{K}^0, \pi^0n, \pi^0\Xi^0\}$, one has

$$\begin{gathered} f_{LS}^{\alpha\alpha;J} = \tfrac{1}{3}\left(2f_{LS}^{J;1/2} + f_{LS}^{J;3/2}\right), \quad f_{LS}^{\beta\beta;J} = \tfrac{1}{3}\left(f_{LS}^{1/2;J} + 2f_{LS}^{;J3/2}\right), \\ f_{LS}^{\beta\alpha;J} = f_{LS}^{\alpha\beta;J} = -\tfrac{\sqrt{2}}{3}\left(f_{LS}^{1/2;J} - f_{LS}^{3/2;J}\right). \end{gathered} \tag{65}$$

Analogous relations, with the substitutions $1/2 \to 0$ and $3/2 \to 2$ of the channel isospins, take place for the channels $\alpha = \{\pi^+\pi^-\}$ and $\beta = \{\pi^0\pi^0\}$ and even values of $L \equiv J$ while, for odd L-values, $f_{L0}^{\alpha'\alpha'',L} = f_{L0}^{1;L}\delta_{\alpha'\alpha}\delta_{\alpha''\alpha}$.

For the channels $\alpha = \{K^+K^-, K^-p, \bar{p}p\}$ and the corresponding ones $\beta = \{K^0\bar{K}^0, \bar{K}^0n, \bar{n}n\}$, one has

$$f_{LS}^{\alpha\alpha;J} = f_{LS}^{\beta\beta;J} = \frac{1}{2}\left(f_{LS}^{0;J} + f_{LS}^{1;J}\right), \quad f_{LS}^{\beta\alpha;J} = f_{LS}^{\alpha\beta;J} = -\frac{1}{2}\left(f_{LS}^{0;J} - f_{LS}^{1;J}\right). \tag{66}$$

In the absence of the Coulomb effects, the unitarity condition (62) allows one to express the amplitude matrix in the channel flavour representation through real symmetric matrices[1] $\hat{\mathcal{K}}_{LS}^J$ or $\hat{\mathcal{M}}_{LS}^J = \hat{k}^L\left(\hat{\mathcal{K}}_{LS}^J\right)^{-1}\hat{k}^L$:

$$\hat{f}_{LS}^J = \left(\left(\hat{\mathcal{K}}_{LS}^J\right)^{-1} - i\hat{k}\right)^{-1} \equiv \hat{k}^L\left(\hat{\mathcal{M}}_{LS}^J - i\hat{k}^{2L+1}\right)^{-1}\hat{k}^L. \tag{67}$$

The second equality in (67) explicitly takes into account the threshold behavior so that the $\hat{\mathcal{M}}$-matrix can be represented by Taylor expansion in the kinetic energy, starting from zero power.

Near threshold, the elements of the diagonal $\hat{\mathcal{M}}$-matrix in the isospin representation are usually parameterized in the so called effective range approximation, taking into account only the first two terms in the Taylor expansion:

$$\mathcal{M}_{LS}^{T;J} \doteq \frac{1}{a_{LS}^{T;J}} + \frac{1}{2}d_{LS}^{T;J}k^2, \tag{68}$$

where $a_{LS}^{T;J}$ is the scattering "length" and $d_{LS}^{T;J}$ is the effective "range" (they have the dimension of a length for $L = 0$ only). Being sensitive to the

[1] In the presence of other open channels in addition to $\{\alpha\}$ or $\{\alpha, \beta\}$, the $\hat{\mathcal{K}}$- and $\hat{\mathcal{M}}$-matrices become complex, when reducing their dimension to one or two.

potential range, the $\hat{\mathcal{M}}$-matrix elements are often called the effective range functions.

Note that neglecting the difference of the channel momenta (e.g., for k sufficiently far above the threshold), the amplitudes $f_{LS}^{T;J}$ satisfy the single-channel unitarity condition and can thus be expressed through the corresponding phase shifts $\delta_{LS}^{T;J}$ according to (63), implying

$$(\mathcal{K}_{LS}^{T;J})^{-1} = k^{-2L}\mathcal{M}_{LS}^{T;J} = k\cot\delta_{LS}^{T;J}. \tag{69}$$

One can improve the isospin relations (64)-(66), applying them to the nearly constant $\hat{\mathcal{M}}$-matrix near threshold (or - to the matrices of scattering lengths and effective radii) rather than to the amplitude matrix $\hat{f}$, thus taking into account the isospin violation only through the mass differences of the particles belonging to the same isospin multiplet, reflected in the difference of the channel momenta.

In the presence of the Coulomb interaction, the $\hat{\mathcal{K}}$- and $\hat{\mathcal{M}}$-matrices enter into the amplitude matrix through a Coulomb modified equation (67) (see, e.g., [21] and references therein):

$$\begin{aligned}\hat{f}_{LS}^{J} &= A_{\rm c}^{1/2}(\hat{\eta})\pi_L^{1/2}(\hat{\eta})\left(\left(\hat{\mathcal{K}}_{LS}^{J}\right)^{-1} - i\pi_L(\hat{\eta})\hat{k}_{\rm c}\right)^{-1}\pi_L^{1/2}(\hat{\eta})A_{\rm c}^{1/2}(\hat{\eta}) \\ &\equiv A_{\rm c}^{1/2}(\hat{\eta})\pi_L^{1/2}(\hat{\eta})\hat{k}^L\left(\hat{\mathcal{M}}_{LS}^{J} - i\pi_L(\hat{\eta})\hat{k}^{2L}\hat{k}_{\rm c}\right)^{-1}\hat{k}^L\pi_L^{1/2}(\hat{\eta})A_{\rm c}^{1/2}(\hat{\eta}),\end{aligned} \tag{70}$$

$$\hat{k}_{\rm c} = A_{\rm c}(\hat{\eta})\hat{k} - 2ih(\hat{\eta})\hat{a}^{-1}, \tag{71}$$

where $\hat{a}$ is a diagonal matrix made from the channel Bohr radii: $a_{\alpha''\alpha'} = a_{\alpha'}\delta_{\alpha''\alpha'}$; $A_{\rm c}(\hat{\eta})$, $\pi_L(\hat{\eta})$ and $h(\hat{\eta})$ are the diagonal matrices with the diagonal elements given by the corresponding function values at the arguments $\eta_{\alpha'}$; the functions

$$\pi_L(\eta) = \prod_{l=1}^{L}(1+\frac{\eta^2}{l^2}), \tag{72}$$

$\pi_0(\eta) = 1$, and

$$\begin{aligned}h(\eta) &= -\ln|\eta| - C + \eta^2\textstyle\sum_{l=1}^{\infty}[l(l^2+\eta^2)]^{-1} \\ &\xrightarrow{\eta\ll 1} -\ln|\eta| - C + 1.20206\eta^2 - 1.03693\eta^4 + 1.00835\eta^6 + \ldots \\ &\xrightarrow{\eta\gg 1} \tfrac{\eta^{-2}}{12} + \tfrac{\eta^{-4}}{120} + \tfrac{\eta^{-6}}{252} + \ldots,\end{aligned} \tag{73}$$

where $C \doteq 0.577216$ is the Euler constant and the arrows indicate low and high η^2 expansions; the η^2 and η^{-2} terms in these expansions are sufficient to achieve better than a percent accuracy at $\eta < 0.3$ and $\eta > 3$, respectively.

In the two-channel case, the explicit matrix inversion in (70) yields

$$f_{LS}^{\alpha\alpha;J} = A_{\rm c}(\eta_\alpha)\pi_L(\eta_\alpha)k_\alpha^{2L}\left[\mathcal{M}_{LS}^{\beta\beta;J} - ik_{\rm c}^{\beta\beta}k_\beta^{2L}\pi_L(\eta_\beta)\right]/D_{LS}^J,$$

$$f_{LS}^{\beta\alpha;J} = f_{LS}^{\alpha\beta;J} = -\left[A_{\rm c}(\eta_\alpha)\pi_L(\eta_\alpha)A_{\rm c}(\eta_\beta)\pi_l(\eta_\beta)\right]^{1/2}(k_\alpha k_\beta)^L\mathcal{M}_{LS}^{\beta\alpha;J}/D_{LS}^J,$$

$$f_{LS}^{\beta\beta;J} = A_{\rm c}(\eta_\beta)\pi_L(\eta_\beta)k_\beta^{2L}\left[\mathcal{M}_{LS}^{J;\alpha\alpha} - ik_{\rm c}^{\alpha\alpha}k_\alpha^{2L}\pi_L(\eta_\alpha)\right]/D_{LS}^J,$$

$$D_{LS}^J = \left[\mathcal{M}_{LS}^{\alpha\alpha;J} - ik_{\rm c}^{\alpha\alpha}k_\alpha^{2L}\pi_L(\eta_\alpha)\right]\left[\mathcal{M}_{LS}^{\beta\beta;J} - ik_{\rm c}^{\beta\beta}k_\beta^{2L}\pi_L(\eta_\beta)\right] - \left(\mathcal{M}_{LS}^{\beta\alpha;J}\right)^2. \tag{74}$$

The multi-channel short-range FSI representation (70-74) was used in [8, 9] for the s-wave amplitudes to calculate correlation functions near threshold.

In the single-channel case, the Coulomb modified amplitude f_{LS}^J in Eq. (70) is expressed through the phase shift δ_{LS}^J according to Eq. (63) and the expression (69) of the effective range functions through the phase shift is modified as:

$$(\mathcal{K}_{LS}^J)^{-1} = k^{-2L}\mathcal{M}_{LS}^J = \pi_L(\eta)\left[A_c(\eta)k\cot\delta_{LS}^J + \frac{2}{a}h(\eta)\right]. \tag{75}$$

Note that a small violation of the isospin symmetry due to the Coulomb interaction can significantly affect the isospin relations (64-66) if applying them to the $\mathcal{M}$-matrix elements in the case, when the latter are small and comparable to this violation.

5.2. Accounting for the inner region

In the following and for Monte Carlo calculations, it is useful to introduce the weight due to the effects of FSI and QS, entering in Eqs. (10), (15), (19) and (52) for the correlation function in case of a universal (independent of the spin projections and intermediate channel flavours) emission function G and the related universal $\mathbf{r}$-separation distribution W_P:

$$\begin{aligned} w(\mathbf{r},\mathbf{k}) &= \tfrac{1}{N(j_1,j_2)}\textstyle\sum_{m_1m_2}\sum_{\alpha'm_1'm_2'}\left|\psi_{-\mathbf{k}}^{\alpha'm_1'm_2';\alpha m_1m_2}(\mathbf{r})\right|^2 \\ &= \tfrac{1}{N(j_1,j_2)}\textstyle\sum_{Sm}\sum_{\alpha'S'm'}\left|\psi_{-\mathbf{k}}^{\alpha'S'm';\alpha Sm}(\mathbf{r})\right|^2 \\ &\to \tfrac{1}{N(j_1,j_2)}\textstyle\sum_{Sm}\sum_{\alpha'm'}\left|\psi_{-\mathbf{k};S}^{\alpha'\alpha;m'm}(\mathbf{r})\right|^2, \end{aligned} \tag{76}$$

where the arrow indicates the case of the conserved total spin S. Averaging the weight over the $\mathbf{r}$-separation of the particle emission points in PRF, one obtains the correlation function:

$$\mathcal{R}(p_1,p_2) = \langle w(\mathbf{r},\mathbf{k})\rangle \equiv \int d^3\mathbf{r}W_P(\mathbf{r},\mathbf{k})w(\mathbf{r},\mathbf{k}). \tag{77}$$

For uncorrelated particles, $w(\mathbf{r},\mathbf{k}) = 1$ and $\mathcal{R} = 1$.

Assuming the characteristic radius r_0 of the $\mathbf{r}$-distribution $W_P(\mathbf{r},\mathbf{k})$ sufficiently larger than the range d of the strong interaction potential, one can choose the separation parameter ϵ substantially smaller than the characteristic source radius r_0. In such a case, one can either approximately neglect the inner contribution of the short-range FSI at $r<\epsilon$, or estimate it using the well-known integral relations for the solutions of a multi-channel scattering problem as described below (see also [8] and references therein).

For $r<\epsilon<r_0$, the separation distribution can be considered independent of $\mathbf{r}$ and taken out of the integral in (77) at its value at the origin (see a discussion of the validity of this approximation in the next Section) to calculate contribution $\mathcal{R}_{<\epsilon}$ to the correlation function from the region $r<\epsilon$ as

$$\mathcal{R}_{<\epsilon} \doteq W_P(0,\mathbf{k})\int_0^\epsilon d^3\mathbf{r} w(\mathbf{r},\mathbf{k}) \equiv W_P(0,\mathbf{k})I(\epsilon,k), \tag{78}$$

where the volume integral $I(\epsilon,k)$ represents an average of the ones at given spin states $\{m_1m_2\}$ or $\{Sm\}$:

$$I(\epsilon,k)=\frac{1}{N(j_1,j_2)}\sum_{m_1m_2} I^{m_1m_2}(\epsilon,k) \equiv \frac{1}{N(j_1,j_2)}\sum_{Sm} I^{Sm}(\epsilon,k). \tag{79}$$

The integrand in the volume integral at a given spin state is the same sum of the contributing scattering wave functions squared as in Eqs. (76), e.g.:

$$I^{Sm}(\epsilon,k)=\int_0^\epsilon d^3\mathbf{r}\sum_{\alpha' S'm'}\left|\psi_{-\mathbf{k}}^{\alpha' S'm';\alpha Sm}(\mathbf{r})\right|^2. \tag{80}$$

The non-symmetrized wave functions are the solutions of the coupled Schrodinger equations

$$\begin{aligned}\mathcal{L}_{-\mathbf{k}}^{\alpha' S'm';\alpha Sm}(\mathbf{r}) \equiv \textstyle\sum_{\alpha'' S''m''}\Big[\big(\nabla^2+k_{\alpha'}^2\big)\delta_{\alpha'\alpha''}\delta_{S'S''}\delta_{m'm''} \\ -2\mu_{\alpha'}V^{\alpha' S'm';\alpha'' S'' m''}(\mathbf{r})\Big]\psi_{-\mathbf{k}}^{\alpha'' S''m'';\alpha Sm}(\mathbf{r})=0.\end{aligned} \tag{81}$$

Forming the identities

$$\partial_{k_{\alpha'}^2}\mathcal{L}_{-\mathbf{k}}^{\alpha' S'm';\alpha Sm}(\mathbf{r})\left[\psi_{-\mathbf{k}}^{\alpha' S'm';\alpha Sm}(\mathbf{r})\right]^* - \partial_{k_{\alpha'}^2}\psi_{-\mathbf{k}}^{\alpha' S'm';\alpha Sm}(\mathbf{r})\left[\mathcal{L}^{\alpha'm';\alpha m*}(\mathbf{r})\right]^*=0 \tag{82}$$

from bilinear products of these equations, the wave functions and their derivatives $\partial_{k^2}=\partial/\partial k^2$ and summing them over all contributing channels $\{\alpha' S'm'\}$, one can express the sum of the wave functions squared at a given $\{Sm\}$ as the gradient of a vector function:

$$\begin{aligned}&\textstyle\sum_{\alpha' S'm'}\left|\psi_{-\mathbf{k}}^{\alpha' S'm';\alpha Sm}(\mathbf{r})\right|^2 \\ &=\nabla\textstyle\sum_{\alpha' S'm'}\Big[\partial_{k_{\alpha'}^2}\psi_{-\mathbf{k}}^{\alpha' S'm';\alpha Sm}(\mathbf{r})\nabla[\psi_{-\mathbf{k}}^{\alpha' S'm';\alpha Sm}(\mathbf{r})]^* \\ &\qquad -[\psi_{-\mathbf{k}}^{\alpha' S'm';\alpha Sm}(\mathbf{r})]^*\nabla\partial_{k_{\alpha'}^2}\psi_{-\mathbf{k}}^{\alpha' S'm';\alpha Sm}(\mathbf{r})\Big].\end{aligned} \tag{83}$$

This expression follows from the hermiticity of the potential $\hat{V} = \hat{V}^+$ and the relation $\mu_{\alpha'}\partial_{k^2_{\alpha'}} = \mu_\alpha \partial_{k^2_\alpha}$.

Note, however, that the sum in the FSI weight (76) is done only over the two-particle states $\{\alpha' S' m'\}$ with the particles belonging to the same isospin multiplets as the particles in the detected channel. Therefore, we have to neglect the contribution of the eventual additional channels also on the right-hand side of (83). Such a truncated equation is exact for $r > d$, when the Schrodinger equations are decoupled and (83) splits into separate equations for each channel $\{\alpha' S' m'\}$. We assume an approximate validity of the truncated Eq. (83) also for $r < d$.

Then, inserting (83) or its truncated form into (80) and using the Gauss theorem, the volume integral $I^{Sm}(\epsilon, k)$ reduces to the difference of the surface integrals $J^{Sm}(r, k)$ on the spheres of the radii $r = \epsilon$ and $r \to 0$. Introducing the functional

$$A_{\alpha'}[\phi, \psi] = \frac{\partial \phi}{\partial k_{\alpha'}} \frac{\partial \psi}{\partial r} - \psi \frac{\partial^2 \phi}{\partial k_{\alpha'} \partial r}, \tag{84}$$

the integral over the surface of a sphere of the radius r can be written as

$$\begin{aligned} J^{Sm}(r,k) &= \textstyle\sum_{\alpha' S' m'} \frac{r^2}{2k_{\alpha'}} \int d\cos\theta d\phi A_{\alpha'} \left[\psi^{\alpha' S' m'; \alpha S m}_{-\mathbf{k}}(\mathbf{r}), \psi^{\alpha' S' m'; \alpha S m *}_{-\mathbf{k}}(\mathbf{r}) \right] \\ &= \textstyle\sum_{L\widetilde{L}} [(2L+1)(2\widetilde{L}+1)]^{1/2} 2\pi r^2 (-1)^{L+\widetilde{L}} \\ &\quad \cdot \textstyle\sum_{\alpha' S' m'} \frac{1}{k_{\alpha'}} A_{\alpha'} \left[\psi^{\alpha' S' m'; \alpha S m}_{k, L' L}(r), \psi^{\alpha' S' m'; \alpha S m *}_{k, L' \widetilde{L}}(r) \right] \\ &\to \textstyle\sum_L (2L+1) 2\pi r^2 \sum_{\alpha' m'} \frac{1}{k_{\alpha'}} A_{\alpha'} \left[\psi^{\alpha' \alpha; m' m}_{k, LS}(r), \psi^{\alpha' \alpha; m' m *}_{k, LS}(r) \right], \end{aligned} \tag{85}$$

where the second equality follows from the expansion of the angular dependence of the wave functions through the D-functions in (37) and the orthogonality relation (48). Averaging Eq. (85) over spin states $\{Sm\}$ of the detected particles and using relations (51), one gets, similar to Eqs (50) and (52):

$$\begin{aligned} J(r,k) &= \textstyle\sum_{\alpha' L' S' L S J} \frac{1}{k_{\alpha'}} \frac{2J+1}{N(j_1,j_2)} 2\pi r^2 \frac{1}{k_{\alpha'}} A_{\alpha'} \left[\psi^{\alpha' \alpha; J}_{k, L' S' L S}(r), \psi^{\alpha' \alpha; J *}_{k, L' S' L S}(r) \right] \\ &\to \textstyle\sum_{\alpha' L S J} \frac{2J+1}{N(j_1,j_2)} 2\pi r^2 \frac{1}{k_{\alpha'}} A_{\alpha'} \left[\psi^{\alpha' \alpha; J}_{k, LS}(r), \psi^{\alpha' \alpha; J *}_{k, LS}(r) \right]. \end{aligned} \tag{86}$$

The arrows in Eqs. (85) and (86) indicate the case of the LS-conservation.

Using the finiteness of the wave functions and their derivatives at $r \to 0$, i.e. $J(0, k) = 0$, we have

$$I(\epsilon, k) = J(\epsilon, k) - J(0, k) = \widetilde{J}(\epsilon, k) \equiv \widetilde{I}(\epsilon, k). \tag{87}$$

The second equality in (87) assumes $\epsilon > d$ so that the surface integral $J(\epsilon, k) = \widetilde{J}(\epsilon, k)$ is given by Eq. (86) with the outer wave functions $\psi_k = \widetilde{\psi}_k$

calculated with the help of the scattering amplitudes according to Eq. (54). Here and below, the tilde denotes the quantities calculated with the help of the outer wave functions even in the inner region.

In case of the LS-conservation, using equation (54), unitarity condition (62) for the elastic $\alpha\alpha$ transition:

$$\Im f_{LS}^{\alpha\alpha;J} = \sum_{\alpha'} k_{\alpha'} \left| f_{LS}^{\alpha'\alpha;J} \right|^2, \tag{88}$$

the Wronskian relation

$$G_L \partial_\rho F_L - F_L \partial_\rho G_L = 1 \tag{89}$$

and the relation $\partial/\partial r \equiv \partial_r = k_{\alpha'} \partial_{\rho_{\alpha'}}$, one obtains: [1]

$$\begin{aligned}
\widetilde{I}(\epsilon, k) = {} & \tfrac{2\pi}{k_\alpha^3} \textstyle\sum_L (2L+1) A_\alpha[F_L, F_L] \\
& + \textstyle\sum_{LSJ} \tfrac{2J+1}{N(j_1,j_2)} \Big\{ \tfrac{2\pi}{k_\alpha} \Re \left(\partial_{k_\alpha} f_{LS}^{\alpha\alpha;J} + k_\alpha^{-1} f_{LS}^{\alpha\alpha;J} \right) \\
& + \tfrac{4\pi}{k_\alpha^2} \Big[\left(A_\alpha[G_L, F_L] - \tfrac{1}{2} \right) \Re f_{LS}^{\alpha\alpha;J} - A_\alpha[F_L, F_L] \Im f_{LS}^{\alpha\alpha;J} \Big] \\
& + \textstyle\sum_{\alpha'} \Big[\tfrac{2\pi}{k_{\alpha'}} \tfrac{\mu_{\alpha'}}{\mu_\alpha} \left(A_{\alpha'}[F_L, F_L] + A_{\alpha'}[G_L, G_L] \right) \left| f_{LS}^{\alpha'\alpha;J} \right|^2 \\
& + \tfrac{4\pi}{k_\alpha} \Im \left(k_{\alpha'} f_{LS}^{\alpha'\alpha:J*} \partial_{k_\alpha} f_{LS}^{\alpha'\alpha;J} \right) \Big] \Big\},
\end{aligned} \tag{90}$$

where the first term represents the pure Coulomb contribution to the inner volume integral:

$$\begin{aligned}
\tfrac{2\pi}{k_\alpha^3} \textstyle\sum_L (2L+1) A_\alpha[F_L, F_L] &= \textstyle\int_0^\epsilon d^3\mathbf{r} \left| \psi_{-\mathbf{k}}^{\alpha;\mathrm{Coul}}(\mathbf{r}) \right|^2 \\
&= \tfrac{4\pi}{k_\alpha^2} \textstyle\sum_L (2L+1) \int_0^\epsilon dr F_L^2.
\end{aligned} \tag{91}$$

In the absence of the Coulomb interaction, $\psi_{-\mathbf{k}}^{\alpha;\mathrm{Coul}}(\mathbf{r})$ reduces to the plane wave $\exp(-i\mathbf{kr})$ and expression (91) coincides with the volume $\frac{4}{3}\pi\epsilon^3$.

Note that on the absence of the J-splitting, one may perform the sum over J in Eq. (90) according to Eq. (53) and make the substitution $\sum_J (2J+1) \to (2L+1)(2S+1)$.

[1] In the first square brackets in Eq. (90), we have omitted the term $[\Im f_{LS}^{\alpha\alpha;J} - \sum_{\alpha'} k_{\alpha'} |f_{LS}^{\alpha'\alpha;J}|^2] \eta \partial_\eta \sigma_L(\eta)$, proportional to the momentum derivative of the Coulomb L-wave phase shift, $\partial_k \sigma_L(\eta) = -k^{-1} \eta \partial_\eta \sigma_L(\eta)$, as this term vanishes due to the unitarity condition (88), To guarantee its vanishing in case of a truncated sum over contributing channels α', one should truncate this sum also in the unitarity condition (88) and use its truncated form to substitute $\Im f_{LS}^{\alpha\alpha;J}$ in Eq. (90). Usually, $k_{\alpha'} |f^{\alpha'\alpha}|^2 \ll |f^{\alpha\alpha}|$ for the rejected channels α' and their contribution to Eq. (90) can be expected small. Note that outside the Coulomb region, $|\eta| > 1$, the magnitude of the factor $\eta \partial_\eta \sigma_L$ is smaller than 0.2, 0.6, 1 and $\ln L$ for $L = 0, 1, 2$ and large L, respectively.

In the considered case of $d < \epsilon < r_0$, both the contributions $\mathcal{R}_{<\epsilon} = \widetilde{\mathcal{R}}_{<\epsilon}$ and $\mathcal{R}_{>\epsilon} = \widetilde{\mathcal{R}}_{>\epsilon}$ of the inner and outer regions to the correlation function are determined by the outer wave functions. They are thus uniquely determined by the scattering amplitudes, independent of a concrete form of the short-range interaction potentials.

Let us now increase the separation parameter ϵ by a small amount $\delta\epsilon$ so that the **r**-separation distribution can be still considered constant for $r < \epsilon+\delta\epsilon$. Then the inner contribution to the correlation function is increased by $\delta\mathcal{R} = \mathcal{R}_{<\epsilon+\delta\epsilon} - \mathcal{R}_{<\epsilon}$ while, the contribution of the outer region is decreased by exactly the same amount so that the complete correlation function remains unchanged. Clearly, it remains unchanged also, when decreasing ϵ by the amount $\delta\epsilon$, guaranteeing that $\epsilon - \delta\epsilon > d$. It is easy to see, however, that one can formally decrease ϵ even below the range d of the strong interaction potential and still have the complete correlation function unchanged if using the outer wave functions also in the inner region.

We may conclude that the complete correlation function is independent of the separation parameter ϵ provided that the **r**-separation distribution can be substituted by a constant for separations $r < \epsilon$. Of course, it is implied that r_0 is substantially larger than the range d of the strong interaction potential so that the **r**-separation distribution can be considered constant for $r < d$; no other information about the short-range interaction potential is required.

In the case, when the short-range FSI can be neglected in all orbital angular momentum waves except for $L = 0$, the volume integral $\widetilde{I}(\epsilon, k)$ is finite even at $\epsilon = 0$. Putting $\epsilon = 0$ and extending the outer weight into the whole inner region, allows one to calculate the correlation function analytically for some simple **r**-separation distributions, e.g., for a Gaussian one [7]. The inner correction is then determined by a limiting value of the s-wave contribution to the volume integral $\widetilde{I}(\epsilon, k)$ at $\epsilon \to 0$, given in Eq. (A.12).

The extension of the outer FSI weight $\widetilde{w}$ down to $r = 0$ is however impractical in case of a non-negligible short-range interaction in higher orbital angular momentum waves since they lead to compensating divergencies at $\epsilon \to 0$ of the $\widetilde{\mathcal{R}}_{>\epsilon}$ and $\widetilde{\mathcal{R}}_{<\epsilon}$, both calculated with the help of the outer wave functions.

Further, to avoid the problem of a slow convergence of the L-expansion of the Coulomb wave function, one can use the analytical expression (33) for the latter down to $\epsilon = 0$ and rewrite the correlation function $\mathcal{R} \doteq \widetilde{\mathcal{R}}_\epsilon$ as

$$\mathcal{R} = \mathcal{R}^{\rm Coul} + \Delta\mathcal{R} \doteq \mathcal{R}^{\rm Coul} + \Delta\widetilde{\mathcal{R}}_\epsilon. \tag{92}$$

For nonidentical particles and spherically symmetric **r**-distribution, the contribution of the short range FSI $\Delta\mathcal{R}$ is given by Eqs. (46), (50) or (52), modified by the following substitution of the scattering wave functions squared:

$$|\psi_{\ldots LS}|^2 \to |\psi_{\ldots LS}|^2 - |F_L(\eta, \rho)/\rho|^2. \tag{93}$$

For $\Delta\widetilde{\mathcal{R}}_\epsilon \doteq \Delta\mathcal{R}$ one has:

$$\Delta\widetilde{\mathcal{R}}_\epsilon = \widetilde{\mathcal{R}}_{>\epsilon} - \mathcal{R}^{\rm Coul}_{>\epsilon} + W_P(0, \mathbf{k})\Delta\widetilde{I}(\epsilon, k), \tag{94}$$

where $\mathcal{R}^{\rm Coul}_{>\epsilon}$ is the outer Coulomb contribution to the correlation function, calculated according to (77) by integrating the Coulomb weight $w^{\rm Coul} = |\psi^{\alpha;{\rm Coul}}_{-\mathbf{k}}|^2$ for $r > \epsilon$. The term $W_P\Delta\widetilde{I}$ represents the inner short-range FSI contribution, where $\Delta\widetilde{I}$ is given by equation (90) with the omitted first term - the inner contribution of the Coulomb distorted plane wave in Eq. (91):

$$\Delta\widetilde{I}(\epsilon,k) = \widetilde{I}(\epsilon,k) - \frac{2\pi}{k_\alpha^3}\sum_L (2L+1)A_\alpha[F_L,F_L]. \tag{95}$$

For identical particles, due to the symmetrization requirement of QS in Eq. (38), only the terms with even $(L+S)$ enter in the above sums over L and S, multiplied by a factor of 2.

Since $\Delta\widetilde{I}(\epsilon,k)$ in (94) represents a volume integral of the additional weight due to the strong FSI over a sphere of the radius ϵ, the Monte Carlo weight, approximately recovering the correlation function in (92), can be defined as (see also equation (17) in [22]):

$$\begin{gathered} w(\mathbf{r},\mathbf{k}) = \widetilde{w}(\mathbf{r},\mathbf{k}) \quad \text{for} \quad r > \epsilon, \\ w(\mathbf{r},\mathbf{k}) = w^{\rm Coul}(\mathbf{r},\mathbf{k}) + \left(\tfrac{4\pi}{3}\epsilon^3\right)^{-1}\Delta\widetilde{I}(\epsilon,k) \quad \text{for} \quad r < \epsilon, \end{gathered} \tag{96}$$

where $\widetilde{w}$ is calculated according to (76) with the help of the outer wave functions.

Since the constant Monte Carlo weight in the inner region is in fact integrated over the true $\mathbf{r}$-distribution, it corresponds to Eq. (94) with $W_P(0,\mathbf{k})$ substituted by a smaller value, determined by the integration of a decreasing $W_P(\mathbf{r},\mathbf{k})$ with the increasing r-separation:

$$W_P(0,\mathbf{k}) \to W_{<\epsilon} = \left(\frac{4\pi}{3}\epsilon^3\right)^{-1}\int_0^\epsilon d^3\mathbf{r}W_P(\mathbf{r},\mathbf{k}). \tag{97}$$

Such a substitution somewhat improves the accuracy of Eq. (94) and extends its validity to lower values of the effective radius r_0.

6. Example calculations

Consider the proton-deuteron correlation function calculated according to Eqs. (92)-(94) in the s-wave approximation for the short-range FSI, using the parametrisation of the $\mathcal{M}$-function in Eq. (75) similar to the effective range approximation in Eq. (68), with the added shape parameter P^S_{0S}:

$$\mathcal{M}^S_{0S} = A_c(\eta)k\cot\delta^S_{0S} + \frac{2}{a}h(\eta) \doteq \frac{1}{a^S_{0S}} + \frac{1}{2}d^S_{0S}k^2 + P^S_{0S}k^4 \tag{98}$$

and the parameters given in Table 2 of [16], obtained from the above expression of the $\mathcal{M}$-function through the phase shift.

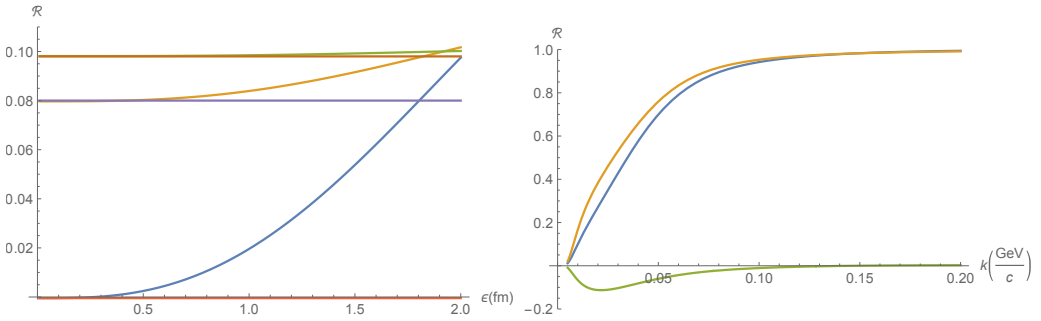

(a) $\mathcal{R}(k)$ at $k = 10$ MeV/c as a function of the separation parameter ϵ; the curves in increasing order correspond to $r_0 = 1.5$, 2, 3 fm

(b) $\mathcal{R}(k)$ at $\epsilon = 1$ fm and $r_0 = 3$ fm (middle blue curve); it represents a sum of the inner Coulomb contribution and the outer, $r > \epsilon$, Coulomb and strong FSI contribution (upper orange curve) and the inner strong FSI contribution (lower green curve)

Fig. 2. The proton-deuteron correlation functions $\mathcal{R}(k)$ calculated in the s-wave approximation for the strong FSI according to Eqs. (92)-(94) (a) and, with the substitution in Eq. (97) (b)

Fig. 2(a) shows the proton-deuteron correlation functions calculated according to Eqs. (92)-(94) in the s-wave approximation for the short-range FSI at $k = 10$ MeV/c and Gaussian source radii $r_0 = 1.5$, 2, 3 fm as functions of the separation parameter ϵ. It demonstrates a weak dependence of the correlation functions on ϵ up to $\epsilon \lesssim r_0$.

Note that the correlation function $\widetilde{\mathcal{R}}_\epsilon$ should be independent of ϵ in case of the nearly constant separation **r**-distribution inside a sphere of a radius larger than the range d of the strong interaction potential. Fig. 2(a) demonstrates that, at $\epsilon \lesssim r_0$, the $\widetilde{\mathcal{R}}_\epsilon$ are rapidly approaching their values at $\epsilon = 0$ fm (the horizontal lines), thus indicating the effective **r**-separation uniform sphere radius comparable or somewhat less than r_0.

In fact, the deviation of the Gaussian **r**-distribution from a constant leads to a power-like ϵ-dependence of the approximate strong interaction contribution $\Delta\widetilde{\mathcal{R}}_\epsilon = \sum_{LS} \widetilde{\rho}_S \Delta\widetilde{\mathcal{R}}_{\epsilon LS}$ to the correlation function at small values of k and ϵ:

$$\Delta\widetilde{\mathcal{R}}_{\epsilon LS} - \Delta\mathcal{R}_{LS} \sim A_c(\eta)(a_L k^L)^2 \epsilon^{3-2L}/r_0^5; \tag{99}$$

recall that the dimension of the scattering "length" $a_L \equiv a_{LS}^J$ is fm^{2L+1}.

Thus, with the decreasing ϵ, the $\Delta\widetilde{\mathcal{R}}_{\epsilon LS}$ approaches a constant as ϵ^3 for $L = 0$, as ϵ for $L = 1$ and, it even diverges as $1/\epsilon$ for $L = 2$. This fact limits practical applicability of Eqs. (92)-(94) for Gaussian-like **r**-distributions to the case of negligible short-range strong FSI with $L > 1$ or - to sufficiently large systems with r_0 essentially larger than the range d of the strong FSI and sufficiently small k. In any case, the applicability of Eqs. (92)-(94) for "small" systems can be improved by the substitution in Eq. (97) and - an optimal choice of $\epsilon \lesssim r_0$ (see below and the next Section).

Fig. 2(b) demonstrates k-dependence of the proton-deuteron correlation

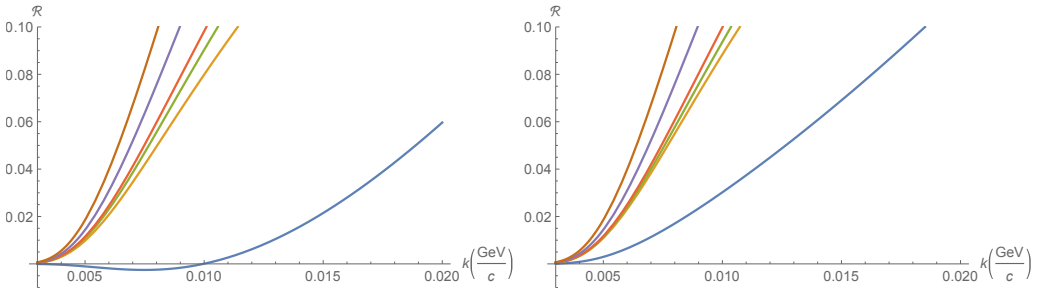

(a) $\mathcal{R}(k)$ at $\epsilon = 0.2$ fm (b) $\mathcal{R}(k)$ at $\epsilon = 1$ fm

Fig. 3. The proton-deuteron correlation functions $\mathcal{R}(k)$ in increasing order for $r_0 =$ 1.5, 2, 2.5, 3, 4, 5 fm, calculated in the s-wave approximation for the short-range FSI according to Eqs. (92)-(94), (97) at $\epsilon = 0.2$ fm (a) and 1 fm (b)

function at $r_0 = 3$ fm - middle curve, calculated in the s-wave approximation for the short-range FSI using Eq. (94) modified by the substitution in Eq. (97). The upper curve represents a sum of the inner Coulomb contribution and the full Coulomb and strong interaction contribution in the outer region ($r > \epsilon$) and the lower one - the inner strong interaction contribution.

The proton-deuteron correlation functions at $r_0 = 1.5$, 2, 2.5, 3, 4 and 5 fm, calculated in the s-wave approximation for the short-range FSI according to Eqs. (92)-(94), (97), are shown in Figs. 3(a) and 3(b) for $\epsilon = 0.2$ and 1 fm, respectively.

Figs. 2(a) and 3 demonstrate a sharp decrease of the correlation function, when decreasing the source radius r_0 from 2 to 1.5 fm. This sharp fall down and unphysical negative values of the correlation function at $r_0 < 1.5$ fm and $k < 10$ MeV/c indicate that the range d of the strong interaction proton-deuteron potential cannot be considered smaller than the characteristic r -separation of particle emitters at so small r_0 values. These figures also demonstrate a substantial, though insufficient, improvement of the correlation function at $r_0 = 1.5$ fm, when increasing ϵ from 0.2 to 1 fm and - a minor effect of this increase at higher values of r_0.

In fact, from the approximate expression for the correlation function at small k (when the short-range FSI is dominated by s-waves) and r_0 significantly smaller than the Bohr radius $|a|$ (see [7] and Eq. (A.12)):

$$\mathcal{R}(k \to 0) \approx A_c(\eta) \sum_S \widetilde{\rho}_S \left[1 + \frac{1}{2} \left| \frac{a^S_{0S}}{r_0} \right|^2 \left(1 - \frac{1}{2\sqrt{\pi}} \frac{d^S_{0S}}{r_0} \right) + \frac{1}{\sqrt{\pi}} \frac{\Re a^S_{0S}}{r_0} \right], \tag{100}$$

as well as, from the fact that the inner correction is proportional to the ratio d^S_{0S}/r_0 in the curved brackets, one may consider the absolute value of the effective range d^S_{0S} as a measure of the strong interaction potential range d at a given total spin S.

Note that $a^S_{0S} = -2.73 \pm 0.10$ fm and $-11.88 \pm^{0.40}_{0.10}$ fm, $d^S_{0S} = 2.27 \pm 0.12$ fm and $2.63 \pm^{0.10}_{0.20}$ fm for the proton-deuteron s-wave scattering with the total

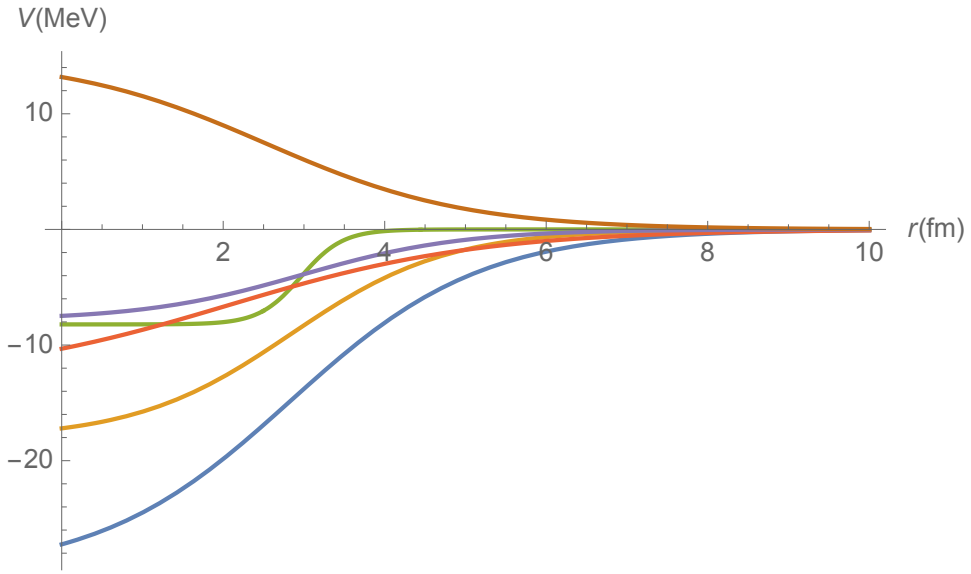

Fig. 4. The proton-deuteron strong interaction Woods-Saxon potentials $V_{LS}(r)$ at given orbital angular momentum L and total spin S obtained in a fit [24] of the low energy phase shifts [16]. In increasing order of the $V_{LS}(0)$, they correspond to L, S values of $0, 1/2$ (blue), $0, 3/2$ (orange), $1, 3/2$ (red), $1, 1/2$ (green), $2, 1/2$ (purple) and $2, 3/2$ (brown).

spin $S = \frac{1}{2}$ and $\frac{3}{2}$, respectively [16] [1].

From the effective range parameters and the fact that a sharp fall down of the correlation function starts at $r_0 \approx 2$ fm, one may conclude that the applicability of Eqs. (92)-(94) requires $r_0 > \left|d_{0S}^S\right| \sim 2.5$ fm.

7. Proton-deuteron correlation from short-range potentials up to d-waves

The approximate calculation of the proton-deuteron correlation function based on the integral relation in Eqs. (92)-(94) can be compared with the exact one, solving Schrodinger equations using available strong interaction potentials up to d-waves [24], shown in Fig. 4. These potentials were obtained by fitting the corresponding phase shifts [16].

Note that according to generalised Levinson's theorem [25], both the s-wave Doublet and Quartet phase shifts from Ref. [16] start at π at zero kinetic energy and the corresponding attractive s-wave potentials support bound states, despite only the Doublet one (^{3}He) is allowed by the Pauli principle.

In Figs. 5-7, we compare the proton-deuteron phase shifts $\delta_{LS}(k)$ from [16] and corresponding effective range functions $\mathcal{M}_{LS}$ calculated according to Eq. (75) with those following from the potentials.

One observes a rough agreement up to $k \sim 150$ MeV/c. Some discrepancies, especially for the Doublet (S=1/2) p-wave, may be related with the

[1] It appears (see Fig. 4) that the proton-deuteron s-wave strong FSI ranges d at $S = 1/2$ and $3/2$ compose 4-5 fm and are somewhat larger than the d_{0S}^S-values.

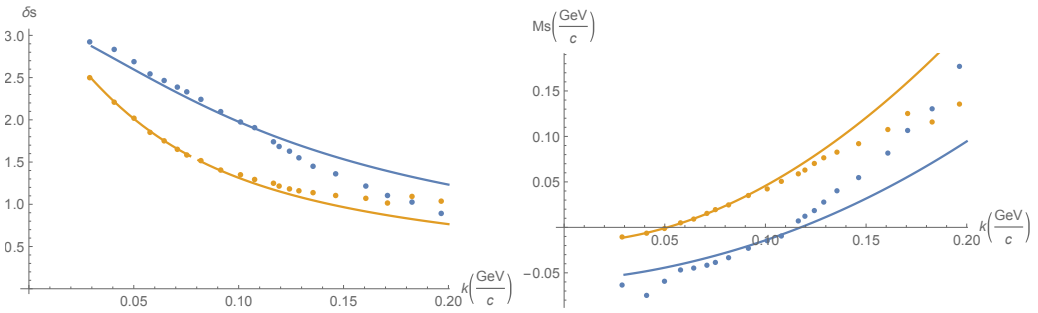

(a) s-wave phase shifts (b) s-wave effective range functions

Fig. 5. The proton-deuteron phase shifts $\delta_{LS}(k)$ from [16] (dots) and calculated from the strong interaction Woods-Saxon potential $V_{LS}(r)$ [24] (curves) at orbital angular momentum $L = 0$ and total spin $S = 1/2$ (blue), $3/2$ (orange); the corresponding effective range functions $\mathcal{M}_{LS}(k)$ are calculated according to Eq. (75)

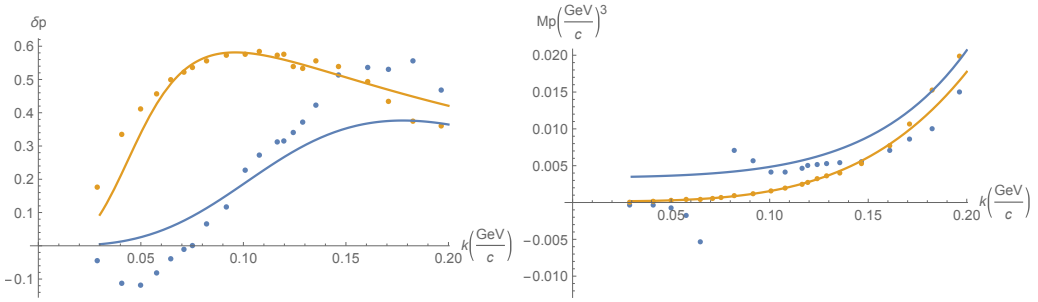

(a) p-wave phase shifts (b) p-wave effective range functions

Fig. 6. The same as in Fig. 5 at $L = 1$ and $S = 1/2$ (blue), $3/2$ (orange)

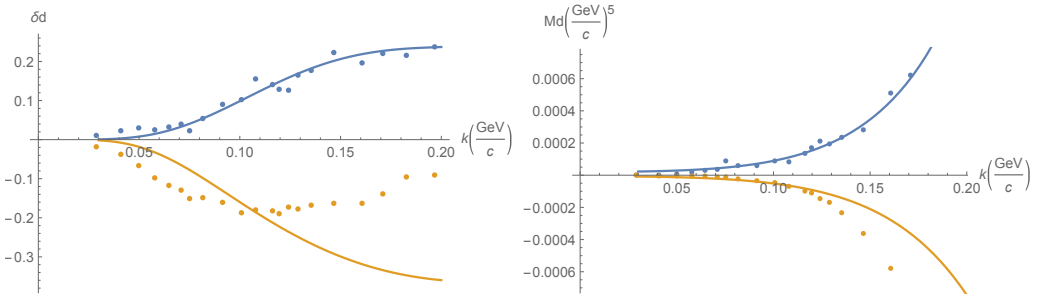

(a) d-wave phase shifts (b) d-wave effective range functions

Fig. 7. The same as in Fig. 5 at $L = 2$ and $S = 1/2$ (blue), $3/2$ (orange)

oversimplified Woods-Saxon potential form, missing the pole at $k \approx 75$ MeV in the cotangent of the phase shift and in the corresponding effective range function. Also, the account of a noticeable inelasticity at $k > 60$ MeV/c [16] may be required.

Since the discrepancies are rather moderate for the Quartet waves, responsible for a dominant strong interaction contribution to the proton-deuteron correlation function, one can use the Woods-Saxon potentials of Ref. [24] for a realistic description of the latter. In figures 8-10, we compare the strong interaction contributions $\Delta\mathcal{R}_{LS}$ to the proton-deuteron correlation function following from these Woods-Saxon potentials with the approximate ones calculated according to Eqs. (92)-(94) at $\epsilon = 1$ fm, modified by the substitution in Eq. (97).

The approximate contributions are quite close or almost coincide with the exact ones for the s-waves and the Doublet p-wave for both Gaussian radii $r_0 = 3$ and 4 fm, while for the other waves they are reasonably close to the latter for $r_0 = 4$ fm only. An excellent agreement of the approximate and exact calculations for the Quartet s-wave and the Doublet p-wave at $r_0 = 3$ fm is caused by a shorter range of the corresponding potentials (see orange and green curves in Fig. 4).

We have checked that, at $\epsilon < 1$ fm, the results of approximate calculations practically coincide with the exact ones for the s-waves and the Doublet p-wave. For the Quartet p-wave and the d-waves, the agreement with the exact calculations is worse. As expected, it is completely destroyed for the d-waves at $\epsilon \to 0$ and somewhat improved by increasing ϵ to make it closer to a given source radius r_0.

One may conclude that for the source radii $r_0 < 4$ fm, the exact calculation based on realistic proton-deuteron potentials is required for a reasonable description of the proton-deuteron correlation function. The resulting strong interaction contribution of the s-, p- and d-waves for $r_0 = 1.5$, 2, 3 and 4 fm is shown in Fig. 11 and the complete correlation function, taking into account the Coulomb FSI, in Fig. 12. One may see that the complete correlation functions at $r_0 = 2 - 4$ fm are quite close to each other.

Conclusions

In this paper, a detailed description of the calculation of a two-particle correlation function at a small relative momentum is given. It is shown that at a characteristic source radius r_0 larger than the range d of the two-particle strong interaction, the exact calculation using the solutions of the scattering problem at given strong interaction potentials reduces to the approximate one based only on the corresponding scattering amplitudes. For correlations of elementary hadrons, the range of the two-particle strong interaction is about one femtometer and the approximate calculation, taking into account the s-wave strong interaction only, is reasonably accurate for sources with the Gaussian radii r_0 on a femtometer level or larger [20]. The

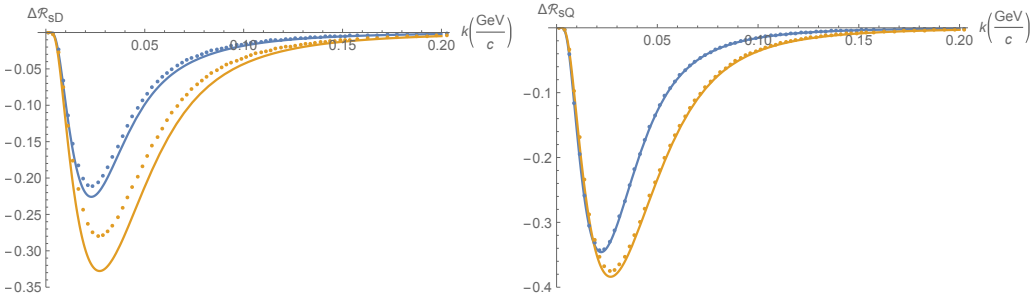

(a) s-wave ($L = 0$) Doublet ($S = 1/2$) (b) s-wave ($L = 0$) Quartet ($S = 3/2$)

Fig. 8. The strong FSI contributions $\Delta\mathcal{R}_{LS}(k)$ at given orbital angular momentum L and the total pair spin S to the proton-deuteron correlation functions calculated from the strong interaction Woods-Saxon potentials [24] (dots) and according to Eqs. (92)-(94) modified by the substitution in Eq. (97) with $\epsilon = 1$ fm (curves) for $r_0 = 3$ fm (orange) and 4 fm (blue)

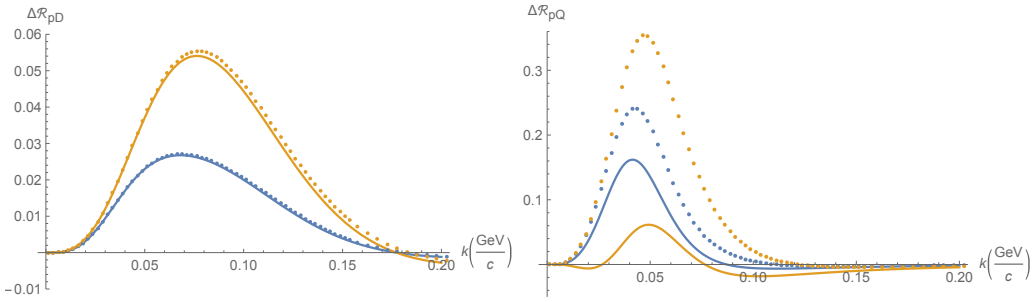

(a) p-wave ($L = 1$) Doublet ($S = 1/2$) (b) p-wave ($L = 1$) Quartet ($S = 3/2$)

Fig. 9. The same as in Fig. 8 for $L = 1$

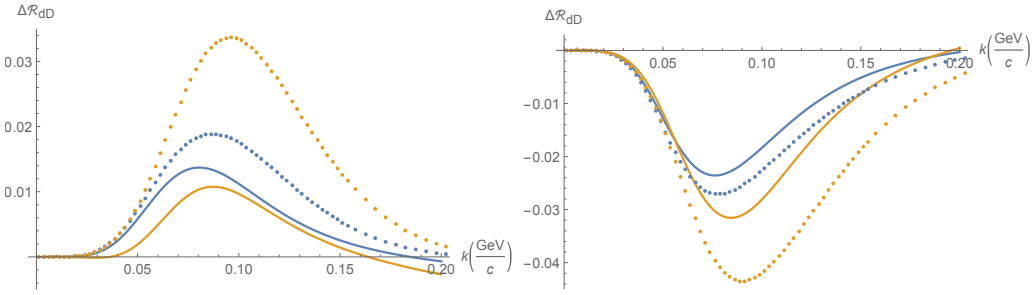

(a) d-wave ($L = 2$) Doublet ($S = 1/2$) (b) d-wave ($L = 2$) Quartet ($S = 3/2$)

Fig. 10. The same as in Fig. 8 for $L = 2$

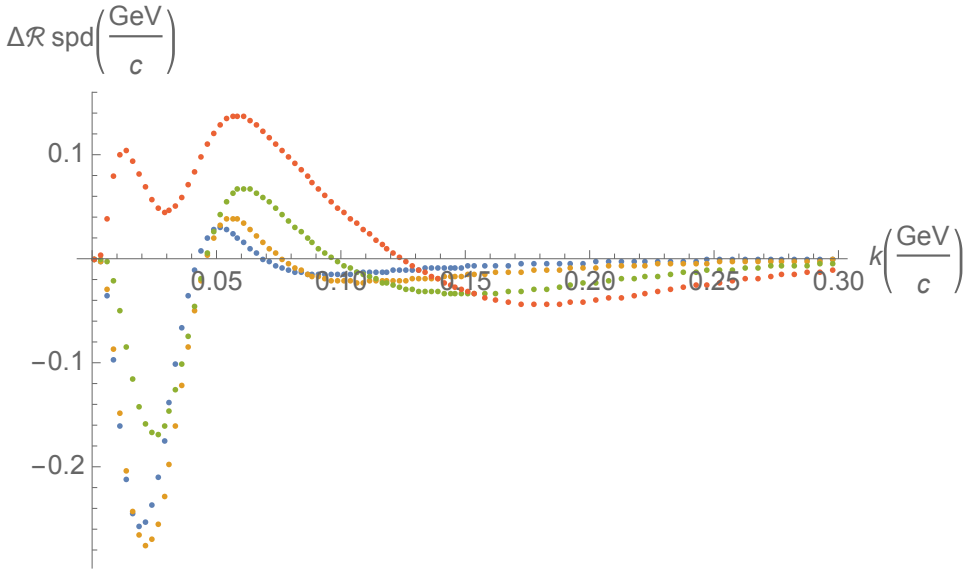

Fig. 11. The strong FSI contribution $\Delta\mathcal{R}_{\rm spd}(k)$ (dots) from the s-, p- and d-waves to the proton-deuteron correlation function calculated from the strong interaction Woods-Saxon potentials [24] for $r_0 = 1.5$ fm (red), 2 fm (green), 3 fm (orange) and 4 fm (blue)

calculation becomes more complicated for correlations involving nuclei due to a larger strong interaction range and a necessity to account for the higher orbital angular momentum waves for the strong interaction even near the threshold [24, 26, 27]. Particularly, comparing the approximate calculations of the proton-deuteron correlation functions with the exact ones, using the Woods-Saxon strong interaction potentials up to d-waves from Ref. [24], we have shown that the former are valid for the radii r_0 larger than 4 fm only and that the assumption of a dominant s-wave strong interaction, used in the analyses of experimental proton-deuteron correlation functions [29,30], is not justified (see also [26, 27]). The correlation involving nuclei may be further complicated by their multi-body nature [28,29]. However, for the source radii r_0 larger than those of the involved nuclei, one may expect the simple two-body approach a valid one [26]. Then, according to Eq. (23), the measured effective hadron-nucleus source radius squared is expressed through the radii r_{0h} and r_{0A} of hadron and nucleus sources as $r_0^2 = (r_{0h}^2 + r_{0A}^2)/2$. Assuming the coalescence formation of a nucleus with the atomic number A (requiring close nucleon emission points in the nucleus rest frame), the corresponding source radius squared is obviously suppressed by a factor of A as compared with the nucleon source radius r_{0N}: $r_{0A}^2 = r_{0N}^2/A$. In particular, the measured proton-deuteron radius r_0 within the two-body coalescence approach becomes $r_0 = \sqrt{3/4}r_{0N}$ [31]. To achieve sufficiently precise description of the correlation functions involving nuclei, one should model more realistic strong interaction potentials rather than the single Woods-Saxon ones [24], a combination of the square wells [26] or the single exponentials [27], describing the available phase shift data in detail. Particularly, the modelled

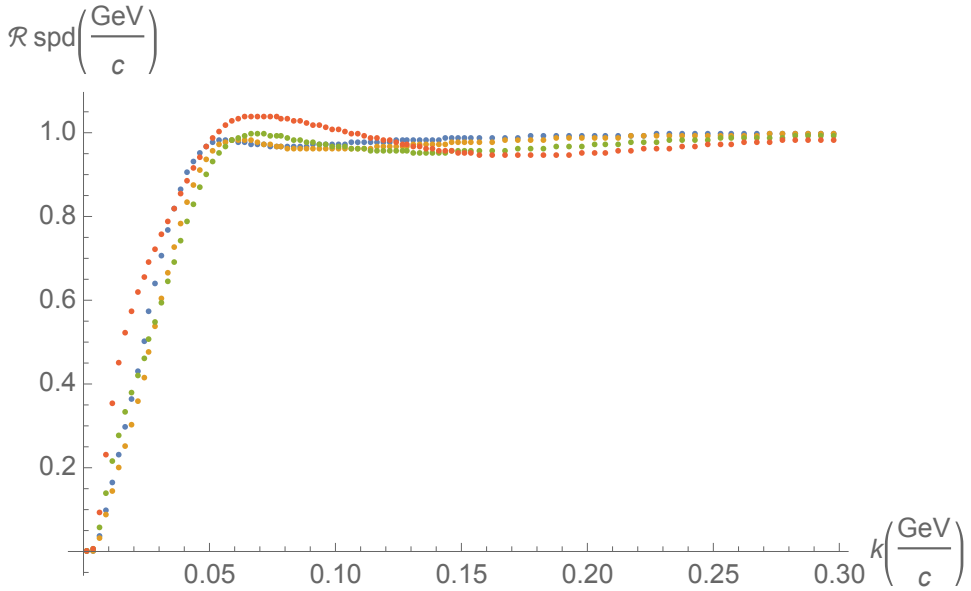

Fig. 12. The same as in Fig. 11 for the complete proton-deuteron correlation functions $\mathcal{R}_{\rm spd}(k)$, taking into account the Coulomb interaction

proton-deuteron potentials should reproduce the poles in the cotangent of the Doublet s- and p-wave phase shifts at $k \sim 12$ MeV/c [32] [1] and $k \sim 75$ MeV/c [16], respectively, as well as the inelasticities. Also, for processes characterised by small source radii, the multi-body effects should be considered.

A. Integral relations

In case of a negligible renormalisation of the amplitudes $f_{LS}^{\alpha'\alpha;J}$ due to the scattering channels different from the channels α' with the particles belonging to the same isospin multiplets as the detected particles in the channel α and - sufficiently far above the threshold (when one can neglect both the difference in channel momenta and the Coulomb FSI), the inner L-wave multi-channel correction integral $\Delta\widetilde{I}$ reduces to a linear combination of the single-channel correction integrals $\Delta\widetilde{I}^T$:

$$\Delta\widetilde{I}(\epsilon,k) = \sum_T \left(C^{Tt}_{T_1t_1;T_2t_2}\right)^2 \Delta\widetilde{I}^T(\epsilon,k), \tag{A.1}$$

[1] In [33], this pole is however found at a negative centre-of-mass energy of -3 keV.

where t_1, t_2 are the projections of the particle isospins T_1, T_2 in the channel α and

$$\begin{aligned}\Delta\widetilde{I}^T(\epsilon,k) = \textstyle\sum_{LSJ} \frac{2J+1}{N(j_1,j_2)} \Big\{ \frac{2\pi}{k} \Re \left(\partial_k f_{LS}^{T;J} + k^{-1} f_{LS}^{T;J} \right) + 4\pi \Im \left(f_{LS}^{T;J*} \partial_k f_{LS}^{T;J} \right) \\ + \frac{4\pi}{k^2} \left[\left(A[C_L, S_L] - \tfrac{1}{2} \right) \Re f_{LS}^{T;J} - A[S_L, S_L] \Im f_{LS}^{T;J} \right] \\ + \frac{2\pi}{k} \left(A[C_L, C_L] + A[S_L, S_L] \right) \left| f_{LS}^{T;J} \right|^2 \Big\} \\ = \textstyle\sum_{LSJ} \frac{2J+1}{N(j_1,j_2)} \frac{2\pi}{k^3} \Big\{ k \frac{d\delta_{LS}^{T;J}}{dk} \\ - \tfrac{1}{2}(-1)^L \left[\sin 2 \left(\rho + \delta_{LS}^{T;J} \right) - \sin 2\rho \right] [1 + b_L(\rho)] \\ - \rho^{-1} c_L(\rho) \left[\cos 2 \left(\rho + \delta_{LS}^{T;J} \right) - \cos 2\rho \right] \Big\},\end{aligned} \tag{A.2}$$

with the same functions b_L, c_L as enter in (A.9) and (A.10) representing polynomials in even powers of ρ^{-1} up to the power $2(L-1)$.

Note that in case of only one channel flavour $\alpha' = \alpha$, (90) reduces to

$$\begin{aligned}\widetilde{I}(\epsilon,k) = \tfrac{2\pi}{k^3} \textstyle\sum_L (2L+1) A[F_L, F_L] \\ + \textstyle\sum_{LSJ} \frac{2J+1}{N(j_1,j_2)} \Big\{ \frac{2\pi}{k} \Re \left(\partial_k f_{LS}^{J} + k^{-1} f_{LS}^{J} \right) + 4\pi \Im \left(f_{LS}^{J*} \partial_k f_{LS}^{J} \right) \\ + \frac{4\pi}{k^2} \left[\left(A[G_L, F_L] - \tfrac{1}{2} \right) \Re f_{LS}^{J} - A[F_L, F_L] \Im f_{LS}^{J} \right] \\ + \frac{2\pi}{k} \left(A[G_L, G_L] + A[F_L, F_L] \right) \left| f_{LS}^{J} \right|^2 \Big\} \\ = \textstyle\sum_{LSJ} \frac{2J+1}{N(j_1,j_2)} \frac{2\pi}{k^3} \Big\{ (2L+1) A[F_L, F_L] + k \frac{d\delta_{LS}^{J}}{dk} \\ + \Big(A[G_L, F_L] - \tfrac{1}{2} \Big) \sin 2\delta_{LS}^{J} + \left(A[G_L, G_L] - A[F_L, F_L] \right) \sin^2 \delta_{LS}^{J} \Big\},\end{aligned} \tag{A.3}$$

where the second equality in (A.3) follows from the single channel unitarity condition, $\Im f_{LS}^J = k \left| f_{LS}^J \right|^2$, and the expression of the amplitudes f_{LS}^J through the phase shifts δ_{LS}^J in (63).

One can further use the recurrence relations for the Coulomb functions $u_L = F_L(\eta,\rho)$ or $G_L(\eta,\rho)$,

$$\begin{aligned} L\partial_\rho u_L &= (L^2+\eta^2)^{1/2} u_{L-1} - (L^2/\rho + \eta) u_L, \\ (L+1)\partial_\rho u_L &= [(L+1)^2/\rho + \eta] u_L - [(L+1)^2 + \eta^2]^{1/2} u_{L+1}, \end{aligned} \tag{A.4}$$

to calculate the derivatives $\partial_\rho u_L$ analytically and thus simplify the numerical calculation of the functionals $A_{\alpha'}$. Omitting the index α' and using the

relation $\partial_k = r\left[\partial_\rho - (\eta/\rho)\partial_\eta\right]$, one arrives at

$$\begin{aligned} A[G_L,F_L] = A[F_L,G_L] + 1 = \rho\tfrac{L^2+\eta^2}{L^2}(G_{L-1}F_{L-1} + G_L F_L) \\ - (L^2+\eta^2)^{1/2}\left(1+\tfrac{\rho\eta}{L^2}\right)(G_{L-1}F_L + G_L F_{L-1}) \\ -\tfrac{L}{(L^2+\eta^2)^{1/2}}F_L G_{L-1} + \tfrac{\eta}{L}\left(\tfrac{L^2}{\rho}+\eta\right)(G_L\partial_\eta F_L - F_L\partial_\eta G_L) \\ +\tfrac{\eta}{L}(L^2+\eta^2)^{1/2}(F_L\partial_\eta G_{L-1} - G_{L-1}\partial_\eta F_L). \end{aligned} \tag{A.5}$$

The functionals $A[F_L,F_L]$ or $A[G_L,G_L]$ follow from (A.5) by substitutions $G_L \to F_L$ or $F_L \to G_L$. Particularly,

$$\begin{aligned} A[F_L,F_L] = \rho\tfrac{L^2+\eta^2}{L^2}(F_{L-1}^2 + F_L^2) - \tfrac{(L^2+\eta^2)[(2L+1)L+2\rho\eta]-L\eta^2}{L^2(L^2+\eta^2)^{1/2}}F_L F_{L-1} \\ +\tfrac{\eta}{L}(L^2+\eta^2)^{1/2}(F_L\partial_\eta F_{L-1} - F_{L-1}\partial_\eta F_L). \end{aligned} \tag{A.6}$$

For $L=0$, one has to put $L=-1$, $u_{-1}=u_0$, $u_{-2}=u_1$ in the r.h.s. of (A.5), (A.6). Particularly, [1]

$$\begin{aligned} A[G_0,F_0] = \rho(1+\eta^2)(G_0F_0 + G_1F_1) \\ -(1+\eta^2)^{1/2}(1+\rho\eta)(G_1F_0 + G_0F_1) + (1+\eta^2)^{-1/2}F_0G_1 \\ -\eta\left(\tfrac{1}{\rho}+\eta\right)(G_0\partial_\eta F_0 - F_0\partial_\eta G_0) \\ -\eta(1+\eta^2)^{1/2}(F_0\partial_\eta G_1 - G_1\partial_\eta F_0). \end{aligned} \tag{A.7}$$

In the absence of the Coulomb interaction or sufficiently far above the threshold, one can make substitutions $\eta \to 0$, $F_L \to S_L$, $G_L \to C_L$ and rewrite (A.5)-(A.7) as

$$A[u_L,v_L] = \rho(u_{L-1}v_{L-1} + u_Lv_L) - L(u_{L-1}v_L + u_Lv_{L-1}) - u_{L-1}v_L, \tag{A.8}$$

where $u_L, v_l = C_L(\rho)$ or $S_L(\rho)$. For $L=0$, one can now retain $L=0$ on the r.h.s. of (A.8) and put $S_{-1}=C_0$ and $C_{-1}=-S_0$. Particularly, for $u_L=v_L=S_L$, we have

$$\begin{aligned} A[S_L,S_L] = \rho - \tfrac{1}{2}(-1)^L[1+b_L(\rho)]\sin 2\rho - \rho^{-1}[a_L(\rho)+c_L(\rho)\cos 2\rho] \\ = \mathcal{O}\left([e(2L+3)^{-1}\rho]^{2L+3}\right), \end{aligned} \tag{A.9}$$

where $a_0=b_0=b_1=c_0=0$, $a_1=-c_1=1$ and, for $L>1$, the functions $a_L(\rho)$, $b_L(\rho)$ and $c_L(\rho)$ are polynomials in even powers of ρ^{-1} up to the power

[1] Putting $G_L=F_L=\phi_l$ or ϕ_l^* in Eqs. (A.5), (A.6) and (A.7) and dividing them by $2k$, one recovers the results for $I_l = \Re A[\phi_l^*,\phi_l]/(2q)$ in Eqs. (21) of [22] if corrected by the substitions $l\eta^2 \to -l\eta^2$ and $\partial_\eta\phi_l \to \partial_\eta\phi_l^*$.

$2(L-1)$; particularly, $a_2 = 3+3\rho^{-2}$, $b_2 = -12\rho^{-2}$ and $c_2 = 3-3\rho^{-2}$. The single-channel equation (A.3) then reduces to

$$\widetilde{I}(\epsilon,k) = \tfrac{2\pi}{k^3}\sum_{LSJ}\tfrac{2J+1}{N(j_1,j_2)}\Big\{k\tfrac{d\delta^J_{LS}}{dk} + \rho - \tfrac{1}{2}(-1)^L[1+b_L(\rho)]\sin 2\left(\rho+\delta^J_{LS}\right) \\ -\rho^{-1}\Big[a_L(\rho)+c_L(\rho)\cos 2\left(\rho+\delta^J_{LS}\right)\Big]\Big\} \\ = \tfrac{2\pi}{k^3}\sum_{LSJ}\tfrac{2J+1}{N(j_1,j_2)}\left[k\tfrac{d\delta^J_{LS}}{dk} + \rho - \tfrac{1}{2}(-1)^L\sin 2(\rho+\delta^J_{LS}) + \sum_{l=1}^{L}\mathcal{O}\left(\rho^{-2l+1}\right)\right], \tag{A.10}$$

with the same functions a_L, b_L, c_L as enter in (A.9). [1]

Note that in the absence of both the Coulomb and strong FSI, the volume integral $\widetilde{I}(\epsilon,k)$ recovers the volume of a sphere of the radius ϵ:

$$\widetilde{I}^{\text{no FSI}}(\epsilon,k) = \tfrac{2\pi}{k^3}\lim_{n\to\infty}\sum_{L=0}^{n}(2L+1)A[S_L,S_L] \\ = \tfrac{2\pi}{k^3}\lim_{n\to\infty}\left[\tfrac{2}{3}\rho^3 + \mathcal{O}\left(\left[e(2n+5)^{-1}\rho\right]^{2n+5}\right)\right] = \tfrac{4}{3}\pi\epsilon^3. \tag{A.11}$$

It should be noted that all the L-contributions to the volume integral $\widetilde{I}(\epsilon,k)$ diverge at $\epsilon\to 0$ except for the s-wave one, whose limiting value takes on the form [8, 9]:

$$\widetilde{I}(0,k) \xrightarrow{L=0} \sum_S\Big\{\tfrac{2\pi}{k_\alpha}\Big[\Re\partial_{k_\alpha}f_{0S}^{\alpha\alpha;S} - \Re f_{0S}^{\alpha\alpha;S}\partial_{k_\alpha}\left(\ln A_{\rm c}(\eta_\alpha)\right)\Big] \\ + 4\pi\sum_{\alpha'}\tfrac{k_{\alpha'}}{k_\alpha}\Big[\Im\left(f_{0S}^{\alpha'\alpha;S*}\partial_{k_\alpha}f_{0S}^{\alpha'\alpha;S}\right) - \tfrac{\eta_{\alpha'}}{A_{\rm c}(\eta_{\alpha'})}\left|f_{0S}^{\alpha'\alpha;S}\right|^2\partial_{k_\alpha}h(\eta_{\alpha'})\Big]\Big\} \\ = -4\pi A_{\rm c}(\eta_\alpha)\Big[\sum_{\alpha'}\left|f_{{\rm c}0S}^{\alpha'\alpha;S}\right|^2\partial_{k_\alpha^2}\mathcal{M}_{0S}^{\alpha'\alpha';S} \\ + \sum_{\alpha'\neq\alpha}2\Re\left(f_{{\rm c}0S}^{\alpha\alpha;S}f_{{\rm c}0S}^{\alpha'\alpha;S*}\right)\partial_{k_\alpha^2}\mathcal{M}_{0S}^{\alpha'\alpha;S}\Big], \tag{A.12}$$

where the matrix $2\partial_{k^2}\hat{\mathcal{M}}^S_{0S}$ at $k=0$ coincides with the matrix of effective radii $\hat{d}^S_{0S}$. The second equality follows from some matrix algebra and explicit account of the Coulomb (Gamow) penetration factors, factoring them out of the amplitudes $\hat{f}^S_{0S}$:

$$f_{0S}^{\alpha'\alpha'';S} = \left[A_{\rm c}(\eta_{\alpha'})A_{\rm c}(\eta_{\alpha''})\right]^{1/2}f_{{\rm c}0S}^{\alpha'\alpha'';S}; \tag{A.13}$$

here the s-wave amplitudes

$$f_{{\rm c}0S}^{\alpha'\alpha'';S} = \left[\left(\hat{\mathcal{M}}^S_{0S} - i\hat{\mathbf{k}}_{\rm c}\right)^{-1}\right]^{\alpha'\alpha''} \tag{A.14}$$

[1] For $L=0$ and 1, the first equality in (A.10) recovers the results of Wigner [12] and Lüders [23] and, the second one coincides with the large-ρ asymptotics in equation (4) of [24], provided the latter is corrected for the lost sign factor $(-1)^L$.

can be considered as the short-range interaction amplitudes affected by the Coulomb forces mainly through the modification of the channel momenta.

Note that both equalities in (A.12) are still valid with a reasonable accuracy, even when truncating the sums over the channel flavours and reducing correspondingly the dimension of the $\hat{\mathcal{M}}_0$-matrix. The latter then becomes a complex matrix and should be substituted by its real part in the second expression in (A.12).

REFERENCES

1. *Kopylov G.I.* Like particle correlations as a tool to study the multiple production mechanism // Phys. Lett. B — 1974. — V. 50. — P. 472–474.

2. *Podgoretsky M.I.* Interference correlations of identical pions. Theory. // Sov. J. Part. Nucl. — 1989. — V. 20. — P. 266–282.

3. *Lednicky R., Podgoretsky M.I.* The interference of identical particles emitted by the sources of different size // Sov. J. Nucl. Phys. — 1979. — V. 30. — P. 432-439; Yad. Fiz. — 1979. — V. 30. — P. 837-844.

4. *Wang F.* Residual correlation in two-proton interferometry from lambda-proton strong interactions // Phys. Rev. C — 1999. — V. 60. — P. 067901-1-3. — arXiv:nucl-th/9907032.

5. *Stavinskyi A., Mikhailov K., Erazmus B., Lednicky R.* Residual correlations between decay products of $\pi^0\pi^0$ and $p\Sigma^0$ systems // — arXiv:07004.3290 [nucl-th].

6. *Adamczyk L. et al.* [STAR Collaboration] Measurement of Interaction between Antiprotons // Nature — 2015. — V. 527. — P. 345–348. — arXiv:1507.07158 [nucl-ex].

7. *Lednicky R., Lyuboshitz V.L.* Effect of the final-state interaction on pairing correlations of particles with small relative momenta // Sov. J. Nucl. Phys. — 1982. — V. 35. — P. 770–778.

8. *Lednicky R., Lyuboshitz V.L., Lyuboshitz V.V.* Final-State Interactions in Multichannel Quantum Systems and Pair Correlations of Nonidentical and Identical Particles at Low Relative Velocities // Phys. Atom. Nucl. — 1998. — V. 61. — P. 2050–2063.

9. *Lednicky R.* Finite-size effect on two-particle production in continuous and discrete spectrum // Phys. Part. Nucl. — 2009. — V. 40. — P. 307–352. — arXiv:nucl-th/0501065.

10. *Goldhaber G., Goldhaber S., Lee W., Pais A.* Influence of Bose-Eistein Statistics on the Antiproton-Proton Annihilation Process // Phys. Rev. — 1960. — V. 120. — P. 300–312.

11. *Kopylov G.I., Podgoretsky M.I.* Correlations of identical particles emitted by highly excited nuclei // Sov. J. Nucl. Phys. — 1972. — V. 15. — P. 219–223.

12. *Wigner E.P.* Lower Limit for the Energy Derivative of the Scattering Phase Shift // Phys. Rev. — 1955. — V. 98. — P. 145–147.

13. *Smith F.T.* Lifetime Matrix in Collision Theory // Phys. Rev. — 1960. — V. 118. — P. 349–356 — Erratum // V. 119. — P. 2098.

14. *Lednicky R.* Correlation Femtoscopy of Multiparticle Processes // Phys. Atom. Nucl. — 2004. — V. 67. — P. 72–82. — arXiv:nucl-th/0305027.

15. *Sinyukov Yu.M., Lednicky R., Akkelin S.V., Pluta J., Erazmus B.* Coulomb corrections for interferometry analysis of expanding hadron systems // Phys. Lett. B — 1998. — V. 432. — P. 248–257.

16. *Arvieux J.* Phase-shift analysis of elastic proton-deuteron scattering cross sections and ^{3}He excited states // Nucl. Phys. A — 1974. — V. 221. — P. 253–268.

17. *Tornow W., Kievsky A., Witala H.* Improved Proton-Deuteron Phase-shift Analysis Above the Deuteron Breakup Threshold and the Three-Nucleon Analyzing-Power Puzzle // Few-Body Systems — 2002. — V. 32. — P. 53–81.

18. *Murano K. et al.* [HAL QCD Collaboration] Spin-Orbit Force from Lattice QCD // Nucl. Phys. A — 1974. — V. 221. — P. 253–268. — arXiv:1305.2293 [hep-lat].

19. *Koonin S.E.* Proton Pictures of High-Energy Nuclear Collisions // Phys. Lett. B — 1977. — V. 70. — P. 43–47.

20. *Gmitro M., Kvasil J., Lednicky R. Lyuboshitz V.L.* On the sensitivity of nucleon-nucleon correlations to the form of short-range potential // Czech. J. Phys. B — 1986. — V. 36. — P. 1281–1287.

21. *Grach I.L., Kerbikov B.O., Simonov Yu.A.* Effective range analysis of low-energy nucleon-antinucleon interaction // Phys. Lett. B — 1988. — V. 208. — P. 309–314. — Nucleon anti-nucleon low-energy interaction in the effective range approximation // Sov. J. Nucl. Phys. — 1988. — V. 48. — P. 609–616.

22. *Pratt S., Petriconi S.* Alternative size and lifetime measurements for high-energy heavy-ion collisions // Phys. Rev. C — 2003. — V. 68. — P. 054901-1–6. — arXiv:nucl-th/0305018.

23. *Lüders G.* Zum Zusammenhang zwischen S-Matrix und Normierungsintegralen in der Quantenmechanik // Z. Naturforschung A — 1955. — V. 10. — P. 581–584.

24. *Jennigs B.K., Boal D.H., Shillcock J.C.* Two-particle correlation functions in the thermal model and nuclear interferometry descriptions // Phys. Rev. C — 1986. — V. 33. — P. 1303–1306.

25. *Sloan I.H.* Two-particle correlation functions in the thermal model and nuclear interferometry descriptions // Phys. Lett. — 1971. — V. 34B. — P. 243–244.

26. *Rzesa W., Stefaniak M., Pratt S.* Theoretical description of proton-deuteron interactions using exact two-body dynamic of femtoscopic correlation method // Phys. Rev. C — 2025. — V. 111. — P. 034903-1-7. — arXiv:2410.13983 [nucl-th].

27. *Torres-Rincon J.M., Ramos A., Rufi J.* A two-body femtoscopy approach to the proton-deuteron correlation function // Phys. Rev. C — 2025. — V. 111. — P. 044906-1-9. — arXiv:2410.23853 [nucl-th].

28. *Viviani M., Konig S., Kievsky A., Marcucci L.E., Singh B., Doce O.V.* Role of three-body dynamics in nucleon-deuteron correlation functions // Phys. Rev. C — 2023. — V. 108. — P. 064002-1-17. — arXiv:2306.02478 [nucl-th].

29. *Acharya S. et al.* [ALICE Collaboration] Exploring the strong interaction of three-body systems at the LHC // Phys. Rev. X — 2024. — V. 14. — P. 031051-1-18. — arXiv:2306.16120 [nucl-ex].

30. *Aboona B.E. et al.* [STAR Collaboration] Light nuclei femtoscopy and baryon interactions in 3 GeV Au+ A u collisions at RHIC // Phys. Lett. B — 2025. — V. 864. — P. 139412-1-8. — arXiv:2410.03436 [nucl-ex].

31. *Mrowczynski S., Slon P.* Hadron-deuteron correlations and production of light nuclei in relativistic heavy-ion collisions // Acta Phys. Pol. B — 2020. — V. 51. — P. 1739-1755. — arXiv:1904.08320 [nucl-th].

32. *Black T.C. Karwowski H.J., Ludwig E.J., Kievsky A., Rosati S., Viviani M.* Determination of proton-deuteron scattering lengths // Phys. Lett. B — 1999. — V. 471. — P. 103-107.

33. *Kievsky A., Rosati S., Viviani M., Brune C.R., Karwowski H.J., Ludwig E.„ Wood M.H.* The Three-Nucleon System Near the N-d Threshold // Phys. Lett. B — 1997. — V. 406. — P. 292-296. — arXiv:nucl-th/9706077.